UNIVERSIDADE FEDERAL DE MINAS GERAIS
Instituto de Geociências
Programa de Pós-Graduação em Geologia

Hugo Marx Gonzaga

STRATIGRAPHY AND DRILLING GEOMECHANICS OF A THICK SALT SECTION: THE ARIRI FORMATION IN THE EASTERN PORTION OF THE SANTOS BASIN

Belo Horizonte

2023

Hugo Marx Gonzaga

STRATIGRAPHY AND DRILLING GEOMECHANICS OF A THICK SALT SECTION: THE ARIRI FORMATION IN THE EASTERN PORTION OF THE SANTOS BASIN

Dissertação apresentada ao programa de Pós-Graduação em Geologia da Universidade Federal de Minas Gerais, como requisito para a obtenção do título de mestre em Geologia Econômica e Aplicada.

Orientador: Prof. Dr. Tiago Amâncio Novo

Belo Horizonte

2023

G642s
2023

Gonzaga, Hugo Marx.

Stratigraphy and drilling geomechanics of a thick salt section [manuscrito] : the Ariri Formation in the eastern portion of the Santos Basin / Hugo Marx Gonzaga. – 2023.

52 f., enc. il. (principalmente color.)

Orientador: Tiago Amâncio Novo.

Dissertação (mestrado) – Universidade Federal de Minas Gerais, Instituto de Geociências, 2023.

Área de concentração: Geologia Econômica e Aplicada.

Bibliografia: f. 46-52.

1. Geologia estratigráfica – Teses. 2. Bacias sedimentares – Teses. 3. Mecânica de rochas – Teses. 4. Perfuração estratigráfica – Teses. 5. Santos, Bacia de – Teses. I. Novo, Tiago Amâncio. II. Universidade Federal de Minas Gerais. Instituto de Geociências. III. Título.

CDU: 551.7(81)

Ficha catalográfica elaborada por Elisabete Quatrini Vieira – CRB-6/2210
Biblioteca "Vitória Pedersoli", Instituto de Geociências da UFMG

UNIVERSIDADE FEDERAL DE MINAS GERAIS

PROGRAMA DE PÓS-GRADUAÇÃO EM GEOLOGIA DO IGC-UFMG

FOLHA DE APROVAÇÃO

Cyclostratigraphy and Drilling Geomechanics of a Thick Salt Section: The Ariri Formation in the Eastern Portion of the Santos Basin

HUGO MARX GONZAGA

Dissertação submetida à Banca Examinadora designada pelo Colegiado do Programa de Pós-Graduação em GEOLOGIA, como requisito para obtenção do grau de Mestre(a) em GEOLOGIA, área de concentração GEOLOGIA ECONÔMICA E APLICADA, pelo Programa de Pós-graduação em Geologia do Instituto de Geociências da Universidade Federal de Minas Gerais.

Aprovada em 24 de julho de 2023, pela banca constituída pelos membros:

Prof. Dr. Tiago Amâncio Novo – Orientador
UFMG

Dr. Humberto Luis Siqueira Reis
HR Consulting

Dr. Filipe Vidal Cunha
Petrobras

Belo Horizonte, 24 de julho de 2023.

AGRADECIMENTOS

À Pró-reitoria de Pós-graduação da UFMG e ao Programa de Pós-graduação em Geologia do Instituto de Geociências da Universidade Federal de Minas Gerais.

À Petrobras e aos colegas da Petrobras, Pedro Francisco Daltoe Cezar, Bruna Souza da Silva, Ana Paula Costa Huguenin, pelo fomento à pesquisa e ao empreendedorismo.

Ao professor Dr. Tiago Amâncio Novo, pela orientação no desenvolvimento do trabalho.

Ao Dr. Tobias Maia Rabelo Fonte Boa, bolsista de pós-doutorado do Projeto IAGEO da UFMG, e aos colegas da Petrobras, Ms. Luciano Costa Gonçalves e Marcelo da Silva Cordeiro, pelas contribuições no tratamento dos dados.

Aos professores Dr. Jose Thomaz Gama da Silva e Ms. Thais Silva, pelo incentivo ao desafio do estudo da língua inglesa.

À minha Família, em especial a minha esposa Lauanna Ferreira Santos, pelo apoio incondicional.

RESUMO

O estudo da estratigrafia e da geomecânica da perfuração dos sais da Formação Ariri foi direcionado ao controle da instabilidade de poços e à redução de tempo não produtivo das operações de perfuração que têm custado milhões de dólares à indústria do petróleo. A área de estudo apresenta sais estratificados em uma zona espessada devido à deformação compressiva dos sais, a halocinese. Foi traçada uma seção 2D que melhor apresentasse continuidade lateral dos refletores sísmicos dos sais e que passasse pela maior quantidade de poços na área. Oito poços foram selecionados para o estudo. Quatro ciclos de deposição de sal de quarta ordem foram interpretados como C1, C2, C3 e C4, da base para o topo da Formação Ariri. O ciclo C1 é o mais espesso dos quatro ciclos e o mais espessado pela halocinese. É também o ciclo mais rico em halita, o que lhe confere sismo-fácies transparente a caótico, e com poucas camadas intercaladas de outros sais. Os ciclos C2 e C3 possuem fácies geológica e sísmica muito semelhantes, com forte sinal sísmico das camadas intercaladas, refletindo sucessões de anidrita, halita e bittern-sais. O ciclo C4 mostrou fácies sísmica caótica e fortes reflexões relacionadas à maior concentração de anidrita e bittern-sais. Os bittern-sais são os sais mais restritos na Bacia de Santos, e mesmo assim podem causar sérios problemas de instabilidade do poço devido à sua alta solubilidade e mobilidade. Eles podem ser lavados pela água não saturada contida do fluido de perfuração, aumentando incontrolavelmente o diâmetro do poço. Por outro lado, uma espessa camada de bittern-sais pode se movimentar rapidamente em condições de alta pressão diferencial, causando o fechamento do poço. A fluência de sal nas camadas de halita do ciclo C1 é a principal causa da instabilidade do poço. A fluência de sal pode levar ao aprisionamento da coluna de perfuração no fundo do poço, o que requer serviços adicionais e eleva muito o tempo e custos da operação. As pressões e temperaturas do poço durante a perfuração em condições de fluência de sal que ocasionaram o aprisionamento da coluna de perfuração foram estudadas e uma curva de tendência foi traçada para ser usada no controle do poço em operações futuras de perfuração de sequencias evaporíticas.

Palavras-chave: Bacia de Santos; estratigrafia; fluência dos sais; Formação Ariri; geomecânica de perfuração.

ABSTRACT

Borehole instability costs millions of dollars to the oil industry as a consequence of the non-productive time of drilling operations. Stratigraphic and drilling geomechanics studies of salts layers of the Ariri Formation provide offer valuable clues to control the instability referred to above. The study area is located in a layered and thickened zone that was created by a compressive halokinetic deformation. A seismic 2D-section was traced passing through a number of wellbores with the best lateral continuity of the salt layers. Eight wellbores were selected for these studies. Major cycles of salt deposition were identified and named as C1, C2, C3, and C4 from bottom to top of the Ariri Formation. The cycle C1 is the most thickened cycle by the halokinesis and the thickest of them. It is halite rich, seismic transparent to chaotical, and shows low interbedded layers. The C2 and C3 cycles have similar geologic and seismic facies and shows strong signal of interbedded layers of anhydrite, halite, and bittern salts. The C4 cycle has chaotical seismic facies and strong reflections that are related to the greater quantity of bittern-salt and anhydrite layers. Salt creeping in the halite layers of the C1 cycle is the main cause of borehole instability. Salt creeping can lead to Bottom Hole Assembly (BHA) stuck, which requires additional services and inflate both operation time and costs. Borehole pressures and temperatures while drilling under salt creeping conditions that produced the BHA stuck were used to draw a Scatter Plot. Statistical analyses have demonstrated a good correlation between pressure and temperature values representing a salt creeping condition that favors BHA stuck. Borehole instability is also related to bittern-salt drilling. Bittern salts are hydrated K-Mg-chlorides that have similar characteristics: high solubility, low density, and low acoustic velocity. Their occurrences are more restricted in the Santos Basin but even so they can cause serious borehole instability problems. Those salts can be washed-out by drilling fluids that enlarge the borehole diameter uncontrollably. On the other hand, a thick layer of bittern salts can creep fast and cause the borehole closure in a high differential pressure condition.

Keywords: Ariri Formation; drilling geomechanics; salt creeping; Santos Basin; stratigraphy.

LISTA DE FIGURAS

LISTA DE TABELAS

SUMÁRIO

1. INTRODUCTION

The Ariri Formation is a halite-rich thick evaporite succession of the Santos Basin, southeastern Brazilian coast (Moreira et al., 2007; Alves et al., 2017). It can reach up to 5,000 meters of evaporite rock thickness in some fault-bounded depressions, although the original thickness of salt is estimated to vary from 1,000 to 3,000 m (Davison et al., 2012). The Ariri Formation became more studied since the year 2000 after the discover of a giant oil and gas reservoir, just below the carbonate layer of the Barra Velha Formation in the Santos Basin (Teixeira et al., 2020). Hundreds of wellbores were drilled through the Ariri Formation during the oil field development, and much information was acquired (Maul et al., 2019).

Oil and gas exploration in deep waters is an extremely complex process and the characterization of the reservoir with little geological data is a challenge (Whitfill et al., 2002). Borehole drilling constitutes an essential component of this process. Its significance is further accentuated when investigating the pre-salt section. A good borehole condition is required to these complex data acquisition. The borehole instability while drilling evaporite rocks is a huge problem that costs the oil and gas industry millions of dollars per year (Poiate et al., 2006). Salt layers are a prominent problem for deep drilling due to their distinguished rheological and compositional characteristics, that usually cause problems and delays during the borehole drilling operation (Lomba et al., 2013). The drilling Bottom Hole Assembly (BHA) stuck by salt creeping, water influxes in the middle of the salt drilling section, and loss of drilling fluid circulation while exiting the salt formation are examples of salt rock interaction that inflate both operation time and costs (Dusseault et al., 2004). Stratigraphy and geomechanics studies can help understand borehole instability to avoid non-productive operation time by controlling unstable drilling of thick salt layers (Dusseault et al., 2004; Costa et al., 2010; Poiate, 2012; Pontes, 2019; Pontes et al., 2021).

The study area is in the eastern portion of the Santos Basin, in a layered, compressed, and thickened zone due to compressive halokinesis deformation (Figure 1A, 1B and 1C - Davison et al., 2012), that includes a developed oil and gas field from where wellbore and 3D seismic quality data were made available by Petrobras for these studies. Seismic and wellbore tie data were used for the interpretation of four thick complete stratigraphic cycles of brine salinity variation during salt deposition, as done by Freitas (2006), Fiduk & Rowan (2015), Rodrigues et al. (2018), Pontes (2019), Teixeira et al. (2020) and Pontes et al. (2021), in similar

areas of the Santos Basin. Those interpreted stratigraphic units were characterized by a succession of anhydrite (CaSO4), halite (NaCl), and bittern salts (K-Mg salts). Bittern salts are highly soluble K-Mg-chlorides as carnallite ($KCl.MgCl_2.6H_2O$), tachyhydrite ($CaCl_2.2MgCl_2.12H_2O$), and Sylvite (KCl) (Jackson and Hudec, 2017). This definition was adopted by Oliveira et al. (2015), Falcão (2017), Yamamoto et al. (2019), Pontes (2019), Maul et al. (2019), and Teixeira et al. (2020) because of their similar low density and velocity characteristics. The interbedded layers of anhydrite and bittern salts were considered by those authors to accurate the velocity model in seismic inversions for several purposes. The succession of those three salts represents the low stand part of a cycle and represents the increasing of the brine salinity in a basin. The high stand part of the cycle is composed of the inverse sequence i.e. bittern salts, halite, and anhydrite representing the decreasing of the brine salinity in a basin. Together they form an entire evaporitic cycle (Freitas, 2006 - Figure 2).

The salt drilling operations of the selected wellbores were geomechanically analyzed using the strategies of Dusseault et al. (2004). These strategies are drilling projects and procedures developed to avoid borehole instability in salt formations by analyzing pressure and temperature data, drilling penetration rates, drilling fluid type, and rock interaction response. These items are also discussed by Lomba et al. (2013) who proposed that bittern-salt drilling interactions be treated as special cases by analyzing its dissolution potential against different types of drilling fluids. In this Brazilian Pre-salt context, stratigraphic and drilling geomechanics studies of salt layers of the Ariri Formation provide insights to control borehole instability.

2. GEOLOGIC AND GEOMECHANIC SETTINGS

The Santos Basin is located in the southeastern margin coast of Brazil. It was formed during the rift of West Gondwana Supercontinent and South Atlantic Ocean opening (Kusznir and Karner, 2007; Aslanian et al., 2009; Moulin et al., 2010). The Santos Basin covers an area larger than 350,000 km², extending from the coastal ranges of the Serra do Mar to the outer limits of the São Paulo Plateau (Pereira and Macedo, 1990; Pereira and Feijó, 1994; Moreira et al., 2007). From south to north, it is limited by the Florianopolis High and the Cabo Frio High, respectively (Garcia et al., 2012; Gamboa et al., 2019). The Santos Basin evolved the stages of syn-rift (Neocomian to Barremian), sag (late Barremian to late Aptian), and drift (Albian to Holocene) and currently it is configured as a passive margin basin (Moreira et al., 2007 - Figure 3).

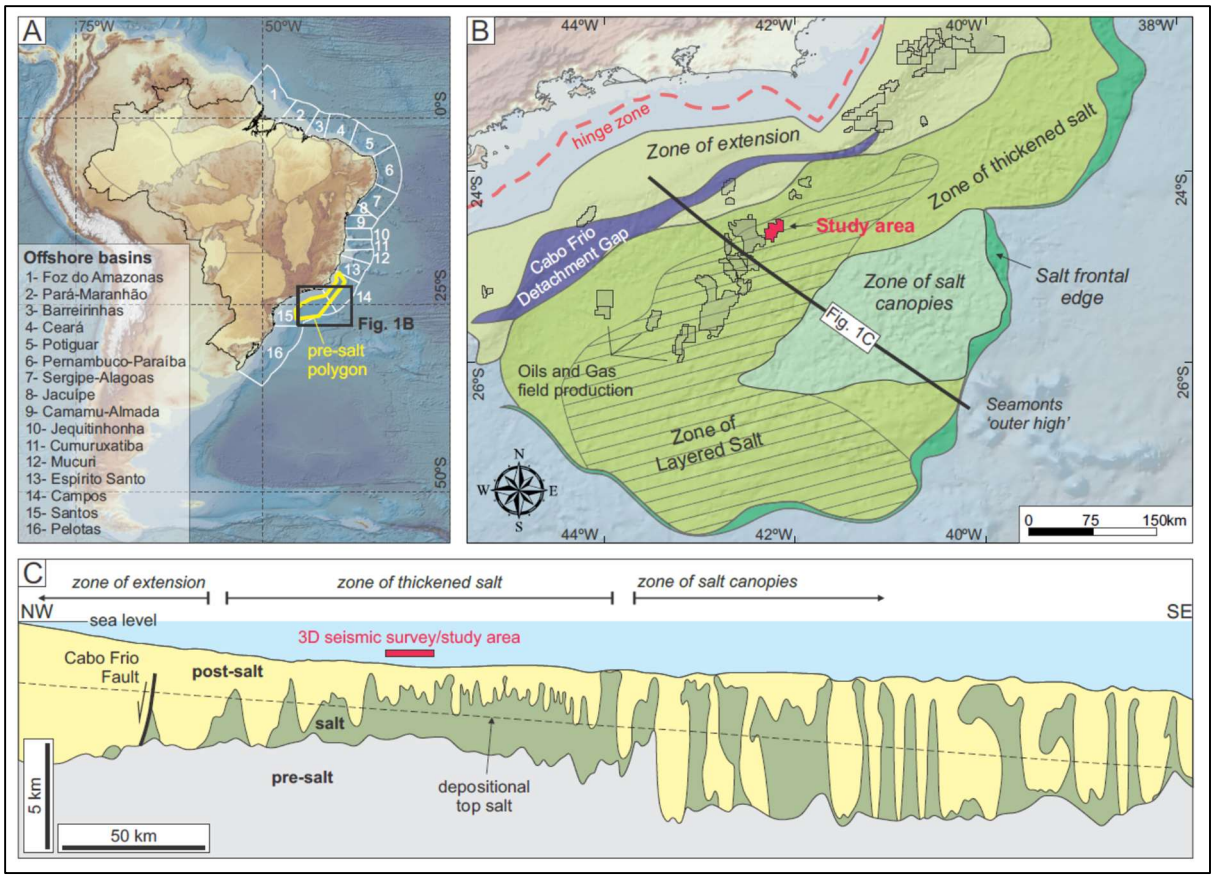

Figure 1A. Study area location in a Brazilian Basin map with emphasis to the pre-salt yellow polygon that is part of the Santos and Campos basins; Figure 1B. Salt-Basing Map showing different structural styles of salt occurrences (modified from Davison et al., 2012). The study area (red) is located in a layered and thickened salt zone; Figure 1C. Geologic cross-section of the study area.

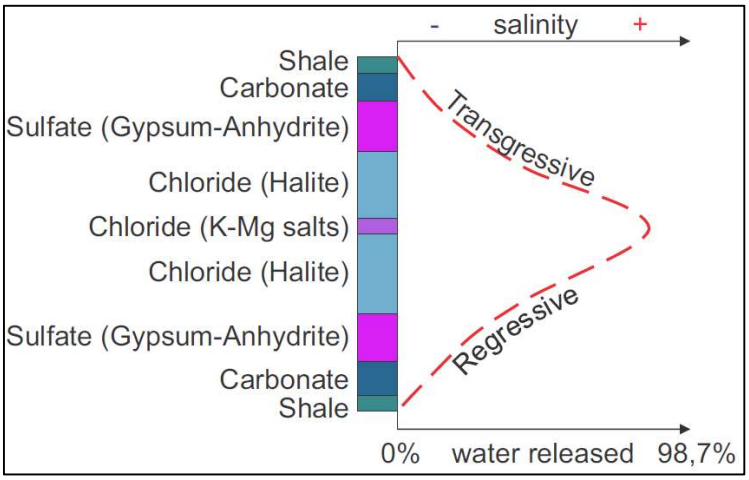

Figure 2. Schematic model of an ideal cycle of deposition of an evaporite sequence (modified from Freitas, 2006).

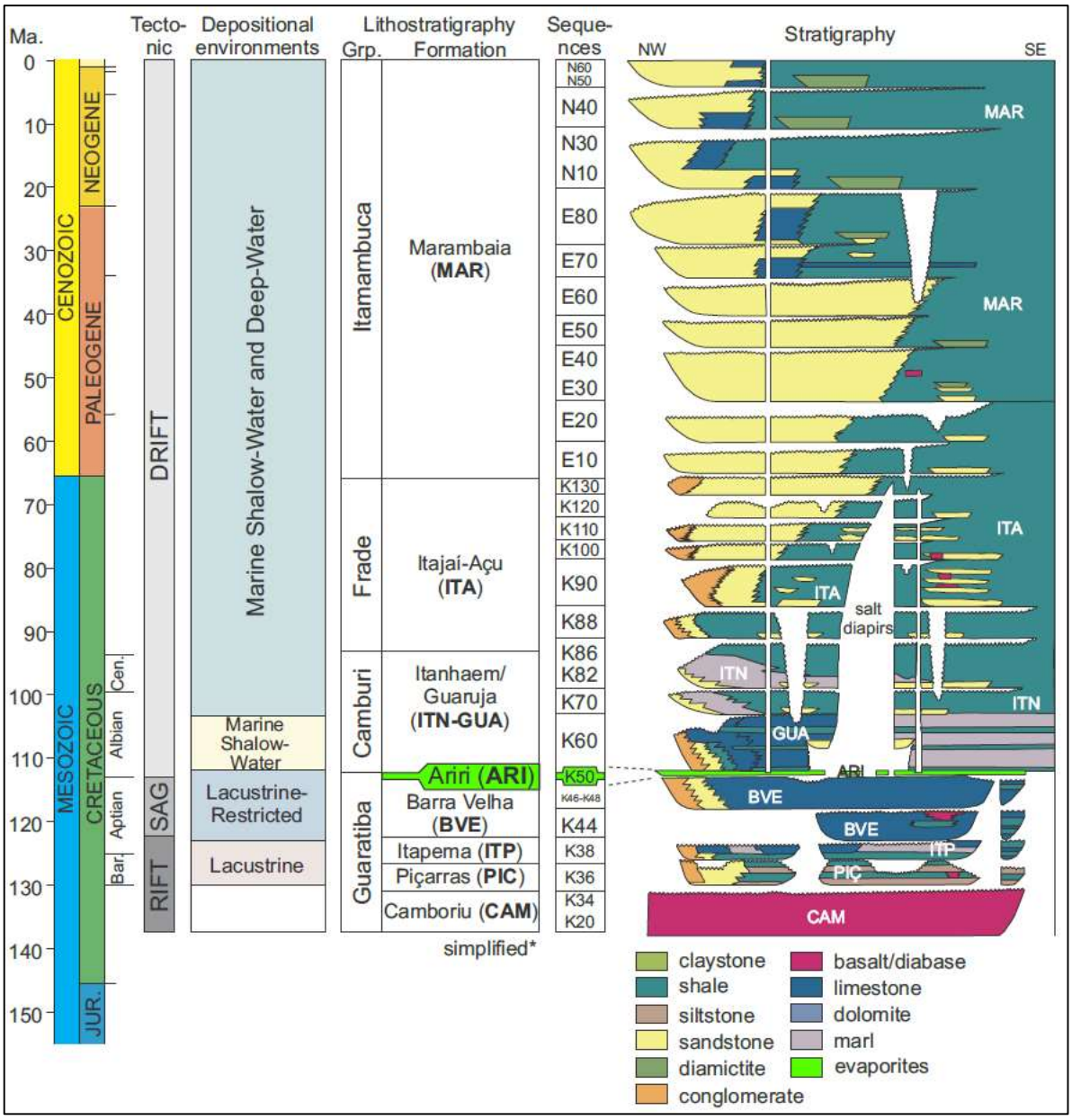

Figure 3. Stratigraphic chart of the Santos Basin (after Moreira et al., 2007). The Ariri Formation was deposited during the Late Aptian.

The Precambrian offshore basement was rifted in the Late Jurassic/Early Cretaceous and formed a series of faults accompanied and covered by volcanic activity along most of the Santos Basin (Moreira et al., 2007). The volcanism was active during the whole rifting evolution and fundamentally influenced the transitional phase. Its influence provided special chemical characteristics to the paleolake system and created an unusual depositional setting. The top of the syn-rift structures includes an extensive SW-NE intrabasinal high called Outer High (Gomes et al., 2012). A wide and elongated SW-NE structural low was formed between the Outer High and the hinge line that favored the development of a structural ramp with carbonate, evaporite,

and huge sedimentary progradation wedge that was emplaced during the Upper Cretaceous. This sedimentation promoted lithospheric load and subsidence of the Santos Basin (Garcia et al., 2012).

The Guaratiba Group is formed by rocks deposited in syn-rift and sag phases of the Santos Basin. From the syn-rift phase, there are the Camboriú, Piçarras, and Itapema Formations that are composed mainly by volcanic, siliciclastic, and carbonate rocks, respectively. From the Aptian-age sag phase, there are the Barra Velha Formation, which is composed mainly of carbonate, and the Ariri Formation, which is comprised of evaporite rocks. The basaltic volcanism of the Camboriú Formation unconformably covers the Pre-Cambrian basement and has been considered the economic basement for petroleum exploration (Moreira et al., 2007; Figure 3).

In the Santos Basin, the carbonate rocks of the Barra Velha Formation contain rich oil pre-salt reservoirs (Szatmari & Milani, 2016). They were probably deposited during the initial stage of a closed evaporite alkaline basin since no marine fossils were identified (Garcia et al., 2012; Farias et al. 2019). The carbonate rocks of the Barra Velha Formation are one of the largest and thickest bodies of nonmarine carbonate worldwide. They are more than 500-m thick (Szatmari & Milani, 2016).

Carbonate layers of the Barra Velha Formation thin and truncate the salt base, thus indicating that a low relief was locally present over the main structural highs. An original depression existed before the salt deposition. This depression was separated from the southernmost Atlantic Ocean by the Walvis Ridge High, which acted as a topographic barrier during the Aptian-age (Davison et al., 2012). Nonetheless, hydrothermal fluids percolated through the volcanic Walvis Ridge fracture zones producing unexpected brine compositions. This alkaline brine was responsible for originating the carbonate rocks of the Barra Velha Formation and the overlying evaporite of the Ariri Formation (Jackson et al., 2000; Farias et al., 2019).

The Ariri Formation was formed by rising the salinity in the sub-sea-level basin at 113 My (Moreira et al., 2007). Freitas (2006) proposed a period of 573 ky for the deposition of those evaporite rocks and described 22 fifty-order cyclostratigraphic units that were associated to the 22 and 39 ky orbital cycles of precession and obliquity. Examples of this include deposits of Lake Assal, Ethiopia (Imbert & Yann 2005), the Messinian evaporites of the Mediterranean

(Clauzon et al. 1996), and the Macleod Basin evaporite of Western Australia (Logan 1987; Table 1). Montaron & Tapponier (2010) proposed a similar period of deposition from numerical modeling studies of evaporation rates.

The Camburí Group is related to the drift evolution in the Albian age after the evaporite deposition. They comprise proximal siliciclastic rocks, shallow-water limestone from the continental shelf, and marl and shale from the distal basin (Moreira et al. (2007). Sequentially, there is the Frade Group, a Neo-Cretacic retrogradational pattern that represents the largest marine transgression in the Santos Basin. It overlays the Camburí Group with deltaic and alluvial siliciclastic proximal fans, marl in the shelf, and shale in the distal basin areas. Ultimately, the Cenozoic sequences of the Itamambuca Group include sandstone and shale that were originated from proximal alluvial fans to distal marine areas, and some occurrences of carbonate platforms (Moreira et al., 2007; Garcia et al., 2012).

Basin	Depositional thickness and interval	Reference	Measurement method
Lake Assal, Djibouti	40-m thick, 1 cm per year	Imbert & Yann (2005)	Physically measured
Mediterranean salt	2-km thick in 300 ky, 0.66 cm per year	Clauzon et al. (1996)	Sr and O isotope stratigraphy
Paradox Basin, Utah	4 cm per year	B. Trudgill (2010)	Counting annual cycles and thickness
Essaouira Basin, Morocco	2 km thick, 0.2 cm per year	Hafid (1999)	Dating the basalt rocks above and below salt
Santos Basin	400–600 ky, 1 cm per year	Freitas (2006)	Milankovitch cycles
Recent salt ponds	<10-m thick, 1 cm per year	Rouchy & Blanc-Valleron (2009)	Physically measured
Macleod Basin, Western Australia	4 mm to 1 m per year over 1,500 years	Logan (1987)	Physically measured

Table 1. Depositional rates of evaporite layers (from Davison et al., 2012).

Distinguished basin wide salt deposits isolated from open-ocean conditions conceal the relationship between salt deposition and sea-level changes (Farias et al., 2019). The brine salinity variation in the basin controls their stratigraphy (Warren, 2006), and the cyclicity of the vertical stack patterns was used by Teixeira et al. (2020) in the evaporite formation division.

Evaporation is the principal factor for concentrating the brine in a basin. At 25°C, gypsum precipitates when the brine salinity becomes five times more concentrated than current seawater. As the brine salinity increases to eleven times the current seawater concentration at 25°C, halite starts to precipitate, and when it becomes up to sixty-three times the current seawater salt concentration at 25°C, the brine favors the deposition of bittern salts (Freitas, 2006; Jackson & Hudeck, 2017). In the opposite way, when water flows somehow to the isolated system of a basin, whether from rain or sea water influx, the brine salinity decreases, returning to precipitate halite, and the onset of a new cycle could be marked when the deposition of gypsum occurs again. Therefore, layers of gypsum or anhydrite, gypsum dehydrated by overburden represent the stage of lowest salinity in the evaporitic basin. On the other hand, bittern-salt layers indicate a stage of highest brine salinity.

Cycles of salt deposition can be characterized in different stratigraphic orders or frequencies. In the Ariri Formation, Freitas (2006) and Rodriguez et al. (2018) mapped fifth-order cycles in addition to the fourth-order cycles that Fiduk & Rowan (2015), Pontes (2019), Teixeira et al. (2020), and Pontes et al. (2021) also documented. Nevertheless, the fourth-order units are better reflected in the seismic expression of the signal and present good association with the borehole geological data. The high-frequency cycles of fifth order cannot be easily identified in seismic scale, in addition to being more difficult to be interpreted and correlate.

The four-fold unit division of the Ariri Formation based on seismic expression of the amplitude was proposed by many authors and converged into a similar definition. Jackson et al. (2015), Rodriguez et al. (2018), and Teixeira et al. (2020) sorted the units from bottom to top and characterized each unit according to their seismic facies expression. The unit 1 is halite-rich, chaotic-stratified, and poor-reflective to transparent because of the low acoustic impedance contrast in this homogeneous rock formation. The unit 2 and 3 have very similar seismic facies presenting high and strong reflective amplitudes that indicate the alternation of anhydrite and bittern-salt layers embedded in halite. The unit 4 is more restricted because of erosion. It is the strongest reflective cycle due to the highest proportion of high-density salts (anhydrite) and low-density salts (bittern salts).

Oliveira et al. (2015), Falcão (2017), Fonseca et al. (2019), Maul et al. (2019), Yamamoto (2019), and Maul et al. (2021) demonstrated the importance of considering salt stratification sections for the correct calibration of seismic velocity model for any purpose including time-depth conversions and geomechanical analyses. However, this is still a new

research area. Stratigraphic studies done by Freitas (2006), Fiduk & Rowan (2012), Jackson et al. (2015), Rodriguez et al. (2018), Pontes (2019), Teixeira et al. (2020), and Pontes et al. (2021) in similar areas of the Santos Basin improved the geologic information of the stratified sequence of the Ariri Formation evaporite. They also showed the substantial importance of refining seismic data processing to improve the accuracy of the subsalt reservoir structures in the seismic images.

Drilling through deep and thick evaporite rocks in an offshore basin is a huge challenge that involves high-cost operations (Costa et al., 2010). Salt creeping and the high solubility properties of salt rocks can cause severe damage to the construction of wellbores (Dusseault et al., 2004). Salt creeping while drilling leads to borehole closure and drilling BHA stuck, that inflate both time and cost of operations. Conversely, uncontrolled borehole enlargement due to salt dissolution by non-saturated water-based drilling fluids can impede casing running and cementation (Lomba et al., 2013).

Halite-rich rocks present different stress conditions than other, sometimes exhibiting identical stresses in all directions, almost equal to the vertical overburden stress. Salt underloading has fluid-like behavior and creeps, equaling all direction stresses in a long-term period (Moiseenkov et al., 2019). At shallow depths, pressures and temperatures are usually lower, but at greater depths, salt creeping can be expected if differential pressures and temperatures properties are not well managed. From 107 to 200 °C, salt creeping can increase abruptly. When the temperature exceeds 200 °C, salt becomes almost completely plastic and flows readily if there is some differential stress (Le Comte, 1965; Barker et al., 1994; Moiseenkov et al., 2019) (Figure 4). Nonetheless, high hydrostatic pressures are used to control salt creeping in the bottom of salt formations. They must be controlled to reduce the risk of lost circulation while exiting salt formations in rubble, sheared or karstic zones underneath the salt section.

Pestana et al. (2018) demonstrate that the present-day geothermal gradient of the Santos Basin shows a thermal anomaly above and below thick salt bodies. They also state that the thermal anomaly above the salt is more difficult to demonstrate due to the lower availability of temperature data of the post-salt rocks. The geothermal gradient published in salt withdrawal is in the 30-34 °C/km range. In the salt layer, it is 11-13 °C/km while in most of the pre-salt section, it is in the 23-26 °C/km range. The geothermal gradient used in these studies

corroborates with Pestana et al. (2018). However, the post-salt section shows a higher range of 33-71 °C/km, that depends on the thickness and depths of the top and the base of the post-salt section. Barker et al. (1994), Poiate et al. (2012), Lomba et al. (2013), among others strengthen that temperature is an essential parameter to help control salt creeping.

Whitfill et al. (2002) discussed how to drill faster, reduce operation costs, and maintain the quality of the borehole gauge. These are achieved using a controlled wash-out technique that requires the displacement of frequent small volumes ("pills"), of seawater to dissolve the salt and enlarge the borehole while drilling. They concluded that oil-based drilling fluids are the most effective fluid to maximize penetration rates of salt drilling.

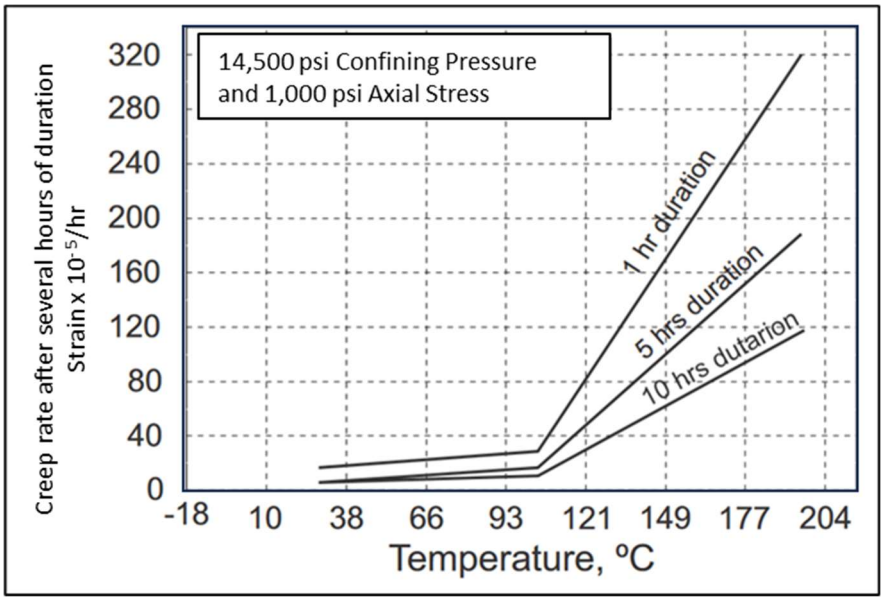

Figure 4. The effect of temperature on salt-creeping rate (after Le Comte, 1965).

Lomba et al. (2013) studied the efficiency and performance of salt drilling when using either water-based or oil-based drilling fluids. They concluded that both fluids dissolve and incorporate the salt in the drilling fluid. The presence of water in the oil-based drilling fluid emulsion contributes to the salt incorporation. Increasing the oil-water ratio in the oil-based drilling fluid and using calcium chloride brine to saturate its water phase reduces the dissolution effect of tachyhydrite. It is important 10^{-5} to notice that if the initial drilling fluid is saturated in a kind of salt (Na^{+}, Ca^{2+}, Mg^{2+} or K^{+}), there will be no dissolution while drilling the equivalent salt rock composition. They also postulated that increasing the drilling rate of penetration and decreasing the drilling fluid flow rate minimizes dissolution by reducing the time between fluid and formation contact.

Salt-creeping rate was studied by Costa et al. (2010). They made some laboratory tests and concluded that tachyhydrite creeps approximately 110 times faster than halite and around 3 times faster than carnallite at 1,450 psi of differential pressure and 86 °C. Dusseaut et al. (2004) showed that the hydrostatic pressure can be adjusted to reduce closure rates by salt creeping. However, limits exist because of potential fracture of the casing shoe at the top of the salt drilling section.

3. DATABASE, METHODS, AND METHODOLOGY

These studies were developed to improve the salt drilling geomechanics knowledge by refining the geological and stratigraphic analyses in the salt-stratified section of the Ariri Formation.

The seismic data used in these studies cover an area of 2,900 km^2 and comprises a 3D Pre-Stack Depth Migration (PSDM) seismic data processed using Reverse Time Migration (RTM) algorithm. Despite the strong halokinesis deformation, it was possible to trace a 2D arbitrary seismic section along the SW-NE trend passing through the largest possible number of drilled wellbores in order to obtain the best lateral continuity in the salt seismic reflectors and avoid salt deformation.

Geologic information from 8 selected wellbores was used to improve the seismic interpretation along the 20-km long section and substantiate the drilling geomechanics analyses. Table 2 shows the official designation of each wellbore given by the ANP, the Brazilian National Petroleum Agency, and the corresponding name used in these studies.

ANP NAME	NAME
3-BRSA-1345-RJS	**Wellbore 1**
9-MRO-2-RJS	**Wellbore 2**
3-BRSA-1343-RJS	**Wellbore 3**
3-BRSA-1356D-RJS	**Wellbore 4**
3-BRSA-1305A-RJS	**Wellbore 5**
3-BRSA-1255-RJS	**Wellbore 6**
7-MRO-7-RJS	**Wellbore 7**
7-MRO-3-RJS	**Wellbore 8**

Table 2. Brazilian National Petroleum Agency (ANP) designation name and corresponding name of the wellbores used in these studies.

The wellbore data set is built with data from two different sources. Drilling parameters, well logs, geologic descriptions of the drilling cuttings samples, geo-pressures, and geo-temperature data are from the drilling acquisition. Some pressure and temperature data such as the Overburden Pressure and Static Rocks Temperature come from the Petrobras data base, that was modelled using the best available techniques. A specific log plot was thoroughly elaborated to analyze occurrences of anomalous behavior while drilling and to better understand the geomechanical state of salt rocks in unstable boreholes.

The cycles of salt deposition were interpreted on vertical logs of the wellbores and on the 2D arbitrary seismic section. The occurrences of borehole instability in the selected wellbores were geomechanically studied and sorted according to the mapped stratigraphic units in the Ariri Formation. The stratigraphic units were interpreted by analyzing the lateral continuity of the seismic reflectors and integrating the wellbore geologic data such as electrical logs and cutting-sample descriptions.

Borehole instability occurrences related to salt-rock interactions were studied using a combined log plot. It is a depth plot composition of electrical logs, drilling parameters, borehole geopressures and geotemperatures classified according to the salt stratigraphic interpretation.

The applied methodology is summarized below:

• Determination of a 2D arbitrary section with best lateral seismic reflectors continuity in the Ariri Formation salt layers and passing by the largest possible number of wellbores.

• Identification of stratigraphic units in the selected wellbores and correlation of the borehole geologic data interpretation to the seismic reflections.

• Interpretation of stratigraphic cycles in the 20-km long seismic arbitrary section.

• Geomechanics analyses of unstable borehole occurrences while drilling.

• Use of stratigraphic and geomechanical analyses to create strategies to avoid non-productive time operations by controlling borehole instability while drilling the salt section.

3.1. Stratigraphy

Major salt stratigraphic units can be mapped for long distances using seismic quality data. In this way, bittern-salt and anhydrite layers embedded in halite layers create distinguished positive and negative amplitude variations. Salt layers thinner than 25 m may not be well seismic recorded since the resolution of this seismic dataset is between 25 and 30 m (Widess, 1973). In such a situation, wellbore data help correct the geologic interpretation.

To simplify the seismic interpretation of the existing salts, three seismic-based facies were used as proposed by Jackson & Hudec (2017) (Table 3): Anhydrite, halite, and bittern salts, respectively. When considering the well-based facies, the anhydrite seismic-based facies include gypsum in addition to anhydrite. The bittern-salt seismic-based facies are composed mainly of carnallite, tachyhydrite, and sylvite. They were put into the same group for seismic-based classification because of their low-density, low-velocity and similar acoustic impedance response. Nevertheless, they can be better identified using gamma ray, resistivity, and sonic borehole logs, according to Mohriak & Szatmari (2009) and Jackson & Hudec (2017).

Seismic-based Facies	Well-based Facies	Chemical Formula	DEN	SON	NEU	GR	RES
Halite	Halite	NaCl	2.03	67	low	low	high
Anhydrite	Anhydrite	$CaSO_4$	2.98	50	low	low	high
Anhydrite	Gypsum	$CaSO_4.2H_2O$	2.35	52	49	low	high
Bittern salts	Carnallite	$KMgCl_3.6H_2O$	1.57	78	65	200	high
Bittern salts	Tachyhydrite	$CaMg_2Cl_6.12H_20$	1.66	88	Low	low	high
Bittern salts	Sylvite	KCl	1.86	74	Low	500	high

Table 3. Well-based classification, seismic-based classification, and other electric well logs properties of evaporites according to Mohriak & Szatmari (2009) and Jackson & Hudec (2017).

In these studies, the seismic interpretation of the evaporite cycles of deposition follows the nomenclature of the four units proposed by Teixeira et al. (2020). They are C1, C2, C3, and C4 from bottom to top of the Ariri Formation.

3.2. Drilling Geomechanics

The wellbore data was evaluated by analyzing the creeping and dissolution process while drilling. After interpreting the stratigraphic units, they were geologically characterized using statistics analysis. Those bittern-salt layers thicker than 20 meters were analyzed

separately because of their high mobility and ease of dissolving by drilling fluids. In addition, their potential to cause borehole instabilities is conspicuously aggravated because of their thickness.

The selected wellbores crossed the Ariri Formation in two different wellbore sections, where drilling geomechanics was studied to understand the specific conditions of the salt-rock interaction in each drilling section. An integrated log plot containing 16 parameters was used to better understand the geomechanical behavior of the salt section when borehole instability occurs. Those parameters were from distinguished data source, classified as drilling parameters, well logs, geopressures, geotemperatures, and geologic data information.

3.2.1. Drilling Parameters

Drilling parameters are data used to control the drilling operations. They include drilling equipment sensors such as Top Drive Drilling, Draw Works Lifting, Pumps and Fluids Tanks (Tavares, 2006; Carrapatoso, 2011; Marques, 2019).

- Weight on bit (WOB): This parameter indicates the drilling string weight on the bit. It represents the downward force exerted by the bit on the rock while drilling.

- Revolutions Per Minute (RPM): Is the speed rotation of the drill bit. It indicates how many rotations per minute the bit is performing.

- Torque (T): This is a measurement of rock resistance to an applied WOB and RPM to the drill bit. It is not a direct controlled parameter by the driller, and it can vary according to different drilled rocks and applied drilling parameters.

- Rate Of Penetration (ROP): Shows how fast is the drilling processes. It is calculated by measuring the length of time required to drill one meter of rock.

- Drilling Fluid Type (DFT): Three different types of drilling fluid are used. The oil-based drilling fluid is a stable emulsion of olefin or paraffin and saturated water, usually in the 60/40 ratio. The water-based drilling fluid is saturated in NaCl. Finally, seawater can be used to drilling sections without fluid return to the rig.

3.2.2. Well Logs

Well logs data are from Log While Drilling (LWD) tools in the BHA. LWD tools are part of the drilling BHA composition that include sensors to measure in real time natural and induced rock characteristics for the geologic interpretation of drilled rocks (Simpson, 2017).

- Gamma Ray (GR): Used to measure the natural gamma rays of the rocks in API units. Each 16.5 API corresponds to a concentration of radioactive elements equal to 1 microgram of radium per ton.
- Resistivity (RES): It measures in ohm.m the electrical resistivity of rocks.
- Sonic or acoustic log (SON): It measures in μs/ft the travel time of an elastic wave through the formation.
- Drilling BHA Vibration (V): Shows the BHA vibrations in G force units. It is measured by accelerometer sensors in the BHA tools of the X, Y and Z axis while drilling. It should be low in a normal condition while drilling halite and bittern-salts layers.
- Bottom-hole Temperature (BHT): This is the temperature of the drilling fluid in °C measured by the BHA tools near to the bit.
- Mechanical Specific Energy (MSE): Express the mechanical work done to excavate a unit volume of rock. It is only used qualitatively as rock trending tool. Proposed by Teale (1965) as $MSE = (WOB/A) + ((120\pi \cdot RPM \cdot T)/(A \cdot ROP))$, where A is the area of the drilling bottom hole in inches.

3.2.3. Geopressures and Geotemperatures

Data derived from Petrobras pre-drilling project database.

- Overburden Pressure (OP): This is the vertical or lithostatic pressure in psi. It is defined as the cumulative weight of overlying seawater sheet, sediments, and rocks with the fluids they contain at a specific depth under the earth surface.
- Hydrostatic Pressure (HP): It is a function of the effective density of a circulating fluid against the formation and its vertical height column. It is given in psi.

- Static-Rock Temperature (SRT): Shows the predicted temperature in °C of the rock on the borehole trajectory in °C. It was modeled by Petrobras pre-drilling staff using temperature measurements that were obtained from other correlated wellbores.

3.2.4. Geological Data Information

- Cutting-sample Geological Description (CGD): It is a wellsite geologist description of the cutting samples, very small fragments from the drilled rocks brought to the rig by the drilling fluid.

- Interpreted Lithology (IL): This is a geologic interpretation from the drilled rocks made by a geologist using electric logs, geological descriptions of the rock samples and drilling parameters.

4. RESULTS

The data analyze start by tracing the arbitrary 2D section passing through the eight selected wellbores (Figure 5). In the sequence, the main cycles of brine salinity variation during salt deposition were identified in each wellbore using the interpreted lithologies. The wellbore-seismic data tie allows the identification of cycles by associating seismic negative amplitude to bittern salts and positive amplitude to anhydrite. Four major cycles of salt deposition were identified in the wellbores. The interpretation of each cycle in the selected wellbores was applied and extrapolated to the entire seismic section by following the corresponding seismic reflector between wells (Figures 6A and 6B).

Figure 7 shows the amount of each group of salt in each cycle for the selected wellbores and for the total analysis. C1, the basal cycle of the Ariri Formation has a strong positive black reflection at its base that is related to the basal anhydrite contact with the carbonate rocks of the Barra Velha Formation. C1 is the thickest cycle. Its thickness varies widely because of the holokinetic deformation. C1 has the highest amount of halite and low quantity of other salts, which is responsible for a transparent and blurred seismic facies appearance in most of the section. There is usually a negative reflection close to its top related to the occurrence of a bittern-salt layer. This layer varies from a few meters to 25 meters in the selected wellbores.

The C2 and C3 cycles are very similar. They have a larger number of interbedded layers of anhydrite and bittern salts, and their thicknesses varies little. C2 is the thinner of them. Strong

reflections are related to layers that are thicker than 10 meters and their little thickness variation is responsible for a good lateral continuity in the seismic section. The C4 cycle presents the larger quantity of interbedded anhydrite and bittern-salt layers. It shows strong and chaotical seismic reflections.

The interpreted cycles show an enrichment of anhydrite and bittern salts from C1 to C4 cycle caused by the increase of high frequency of lithologic variations. Anhydrite and bittern-salt layers do not have a wide thickness variation in the major stratigraphic cycles. Their thickest layers in the studied wellbores have about 70 meters and layers thicker than 20 meters were found in all the interpreted cycles of the Ariri Formation (Figure 8).

All the selected wellbores present static rock temperatures lower than 93°C at the bottom of the Ariri Formation (Table 4). Shallow seabed and thick post-salt section can also contribute to increase the overburden pressure on salt formations as their static rock temperatures, elevating the risks of salt creeping.

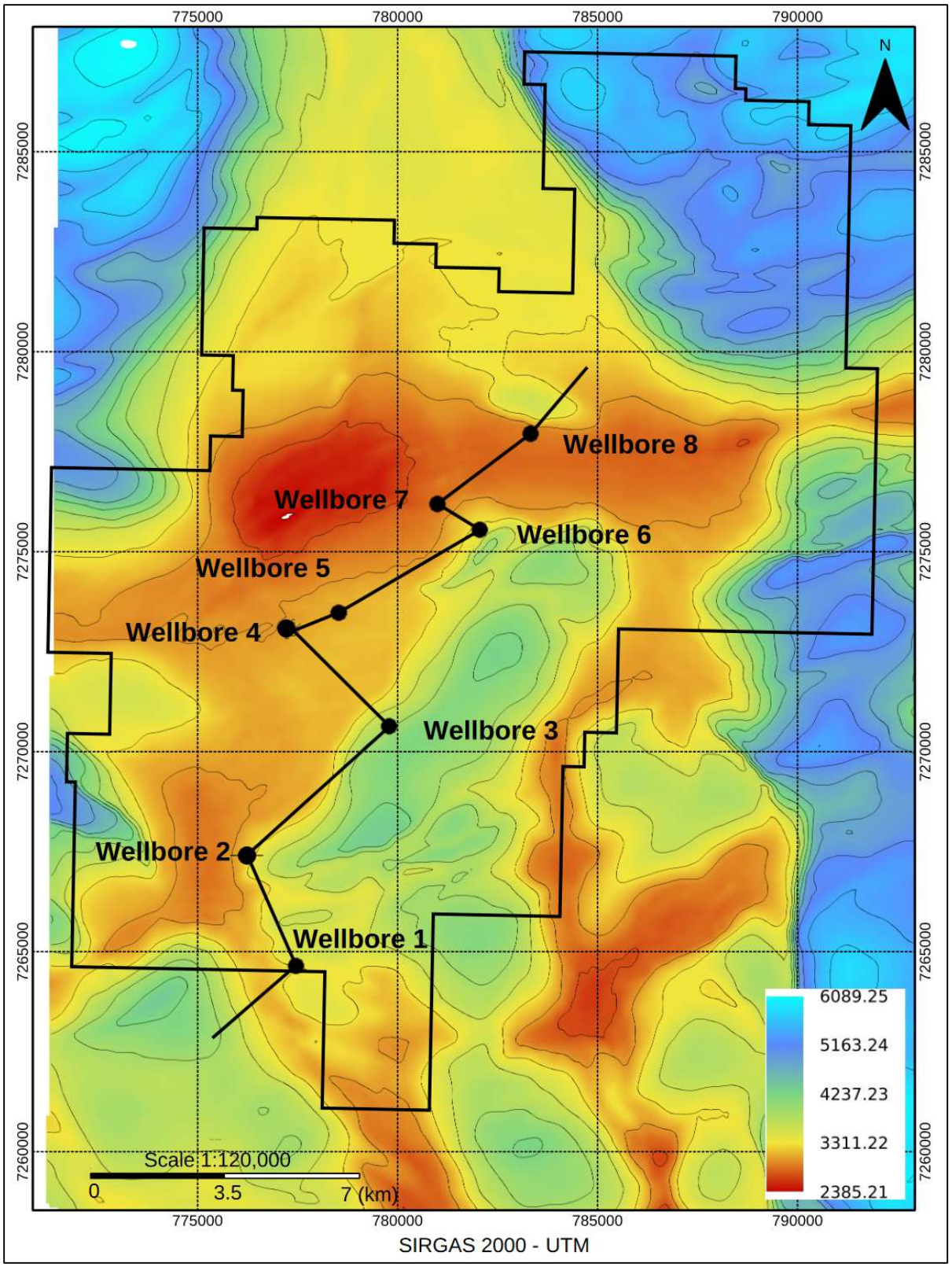

Figure 5.Isopach map of the top of the Ariri Formation in the study area (Mero Oil Field black outline) with the location of the seismic section passing through the selected wellbores from 1 to 8.

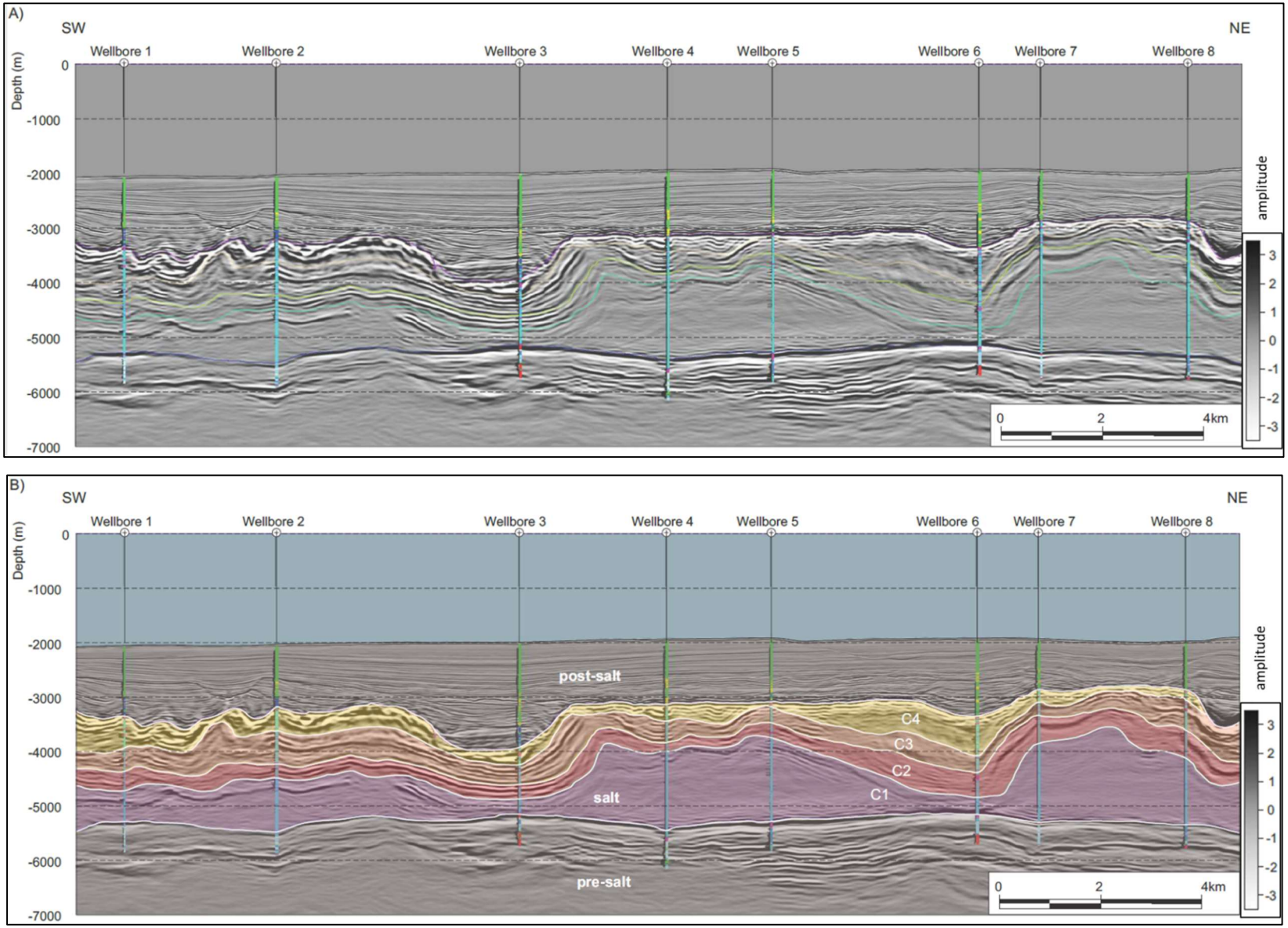

Figure 6A. Arbitrary section across the 8 selected wellbores. Figure 6B. Seismic interpretation of the four interpreted cycles on the Ariri Formation.

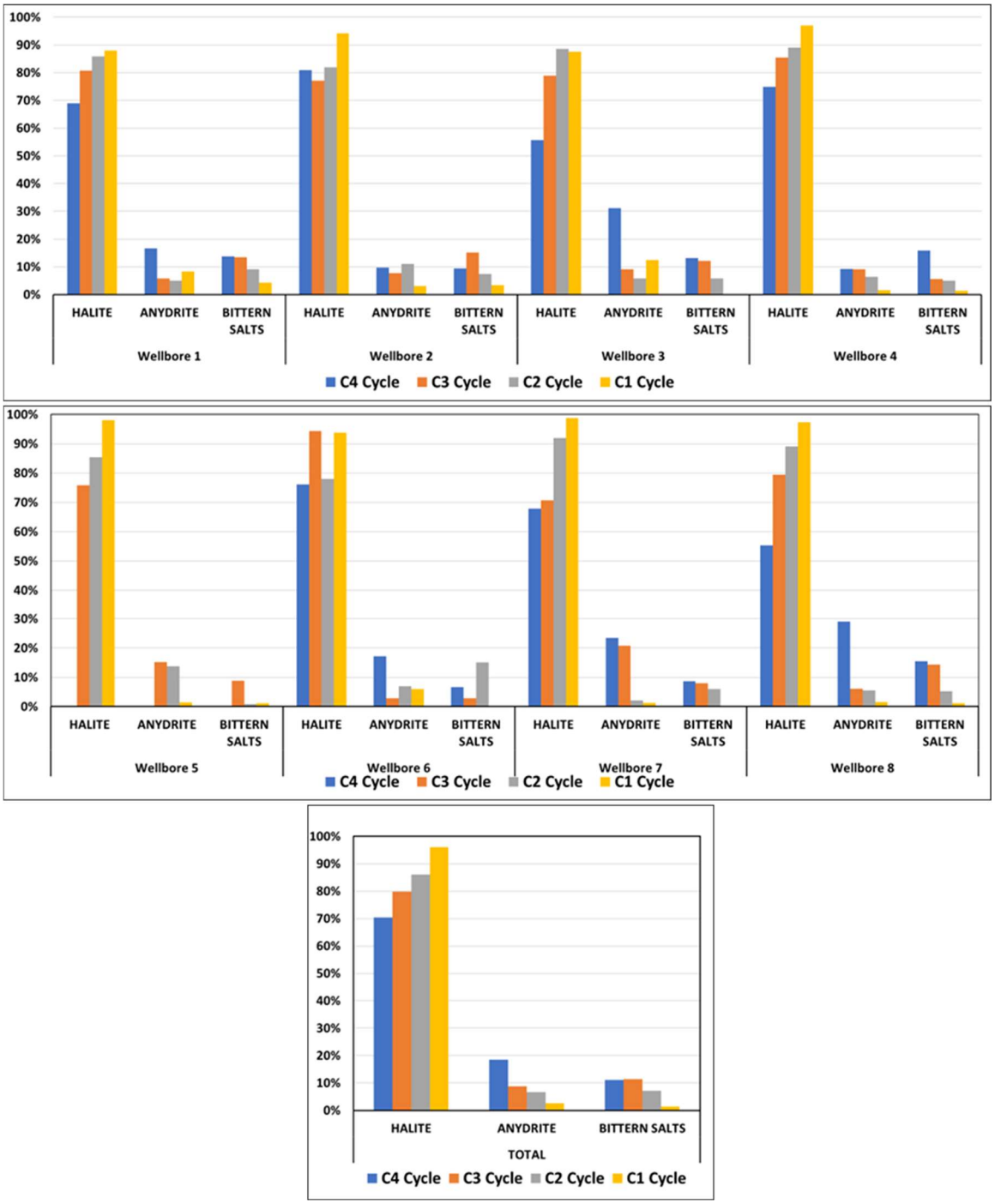

Figure 7. Rock ratio of each interpreted cycle for the selected wellbores and for the total.

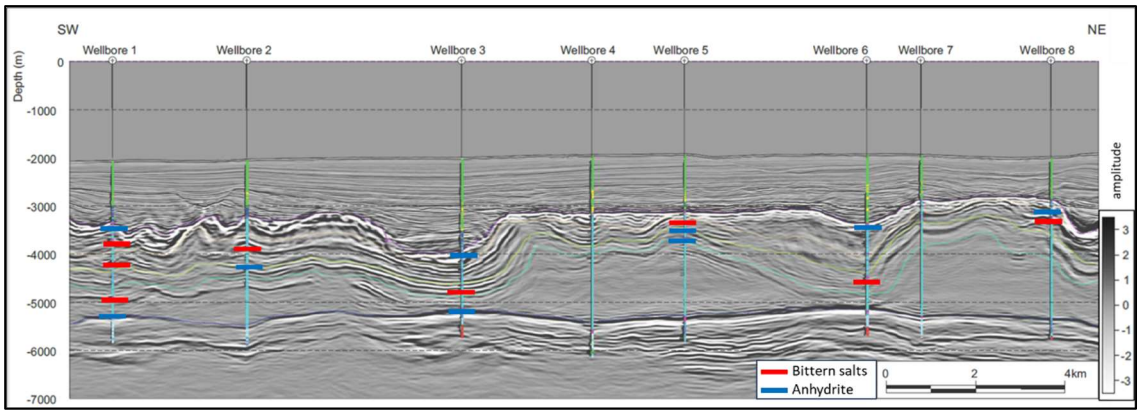

Figure 8. Interpreted 2D section showing bittern-salt layers (red flag) and anhydrite layers (blue flag) thicker than 20 meters in the selected wellbores.

WELLBORE	1	2	3	4	5	6	7	8
Seabed (m)	2,116	2,056	2,018	2,003	1,975	1,975	1,989	1,945
Pos-salt Thickness (m)	1,302	1,179	1,908	1,120	1,131	1,456	864	1,043
Salt Thickness (m)	1,970	2,222	1,271	2,292	2,130	1,702	2,442	2,395
Top Salt Depth (m)	3,418	3,235	3,926	3,123	3,106	3,431	2,853	2,988
Top Salt Temperature (°C)	57	54	67	52	57	59	46	53
Base Salt Temperature (°C)	79	82	81	83	85	77	78	80
Base Salt Depth (m)	5,388	5,457	5,197	5,415	5,236	5,133	5,295	5,383
Temperature Gradient on salt section (°C/Km)	11.16	12.60	11.01	13.52	13.14	10.57	13.10	11.27

Table 4. Thicknesses and temperatures of the selected wellbores.

Occurrences of borehole instability in the salt section (Figure 9) were classified according to the stratigraphic characterization. They are described below.

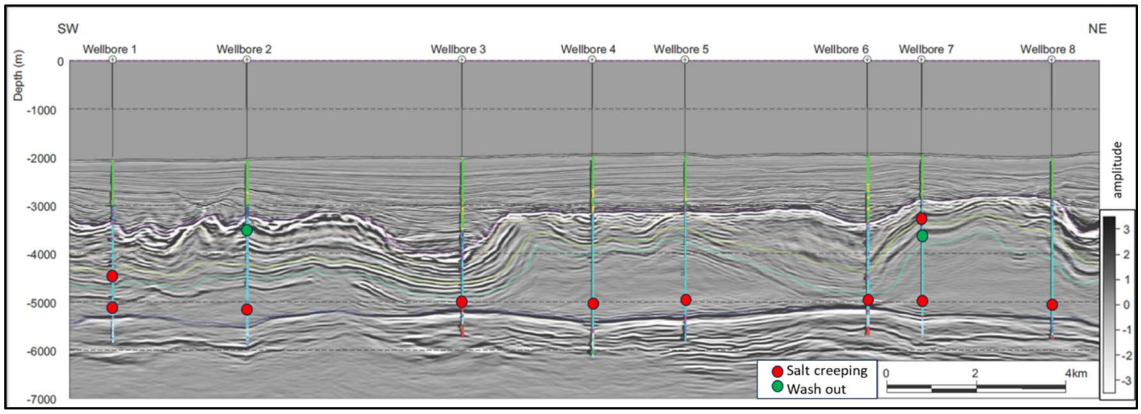

Figure 9. Interpreted 2D section showing the borehole instability events. The red circles represent events of BHA stuck attributed to salt creeping and the white circle represents borehole uncontrolled enlargement due to salt dissolution.

4.1. Wellbore 1

The main events of borehole instability of the Wellbore 1 in the Ariri Formation are two occurrences of BHA stuck in a halite layer, that were associated to salt creeping when drilling the 16-inch section using oil-based drilling fluid. The first event was a slight BHA stuck in a halite layer of the C2 cycle, and the second was a severe BHA stuck in the C1 cycle (Figure 10).

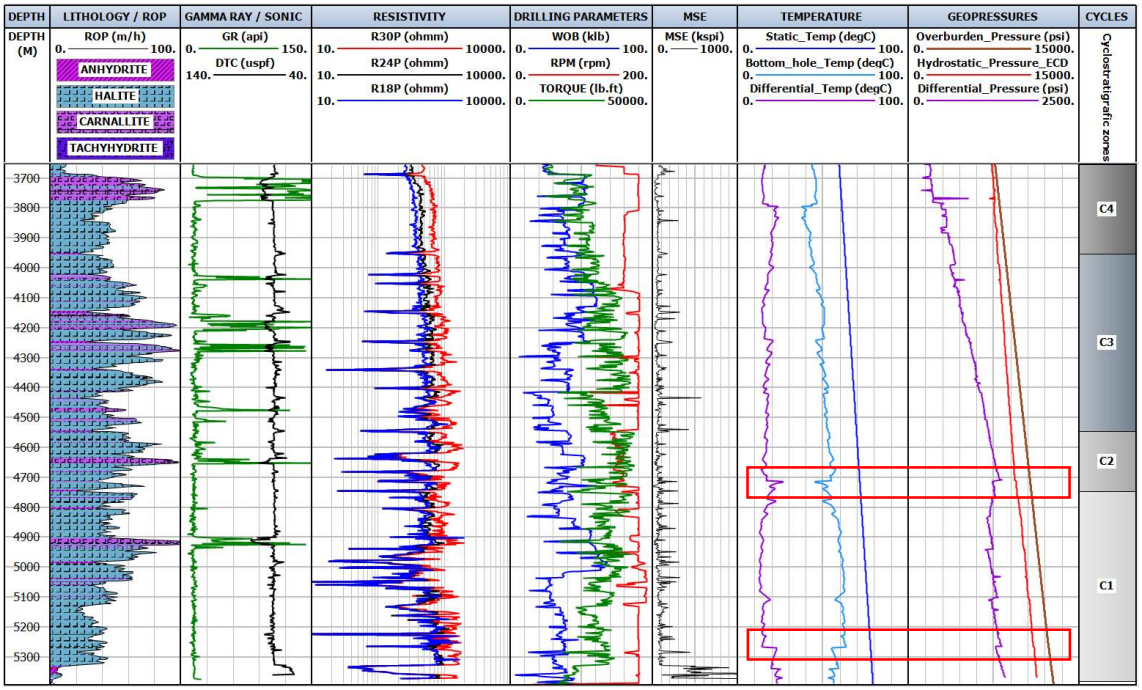

Figure 10. Log plot of the 3,700 to 5,300 m interval of the 16-inch section the Wellbore 1. The red boxes show the interval of BHA stuck by salt creeping in the C2 and C1 cycle.

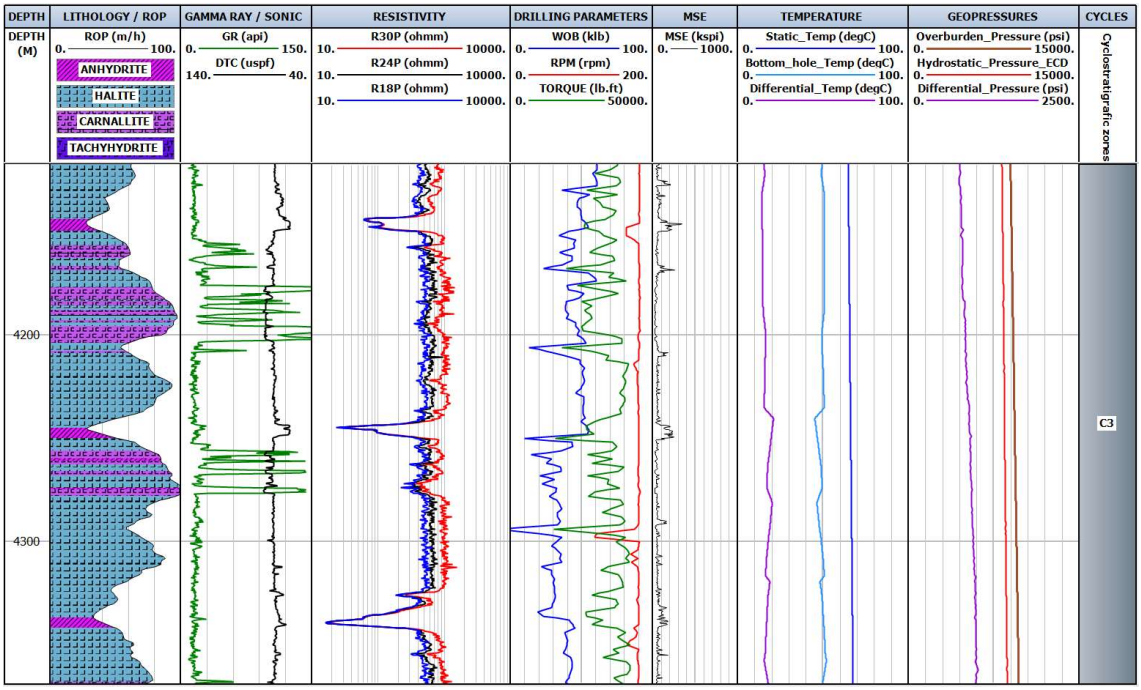

Figure 11. Log plot of the 4,100 to 4,400 m interval of the Wellbore 1. Bittern salts of the C3 cycle.

The Figure 10 is composed by 9 tracks. Track 1 to 5 contain the most important perameters used in the lithologic interpretation. Track 1 represents the measured depth, and the track 2 is composed by the drilling ROP, shaded by the IL. Low ROP values are associated to anhydrite, and high ROP values, to bittern salts. GR and SON logs are in the track 3 and three RES logs in the track 4 (R18P, R24P, and R30P). Those are 3 different arrays of the resistivity log-tool, that measure the formation resistivity response on different investigation radii from the tool sensors. Track 5 has WOB, T, and RPM, that are drilling parameters used in the lithological interpretation of the drilled rocks. For anhydrite, there was necessary to apply higher WOB and high values of T were registered due to its higher hardness than halite and bittern salts, where usually there was necessary low WOB to drill.

Red boxes mark two stuck BHA events on Figure 10, tracks 7 and 8, where the highest differential pressure and lowest differential temperatures were registered while drilling. MSE in the track 6 is also used to support the lithological interpretation, mostly by its huge difference response between halite (lower values) and anhydrite (higher values). Events of BHA stuck happened in halite layers at the bottom of the C2 and C1 cycle, which are represented on the track 9.

Figure 11 is a 300-meters log plot of the C3 cycle in Wellbore1 where anomalous low resistivity values occur in anhydrite layers. Expressive bittern salts interbedded with halite were also interpreted in this drilling section.

4.2. Wellbore 2

Figure 12 shows a 26-inch section where an anomalous low resistivity values in a 15-meter thick layer of carnallite was drilled using seawater as the drilling fluid. This was considered as an unstable borehole condition, for being interpreted as an uncontrolled enlarged borehole gauge interval.

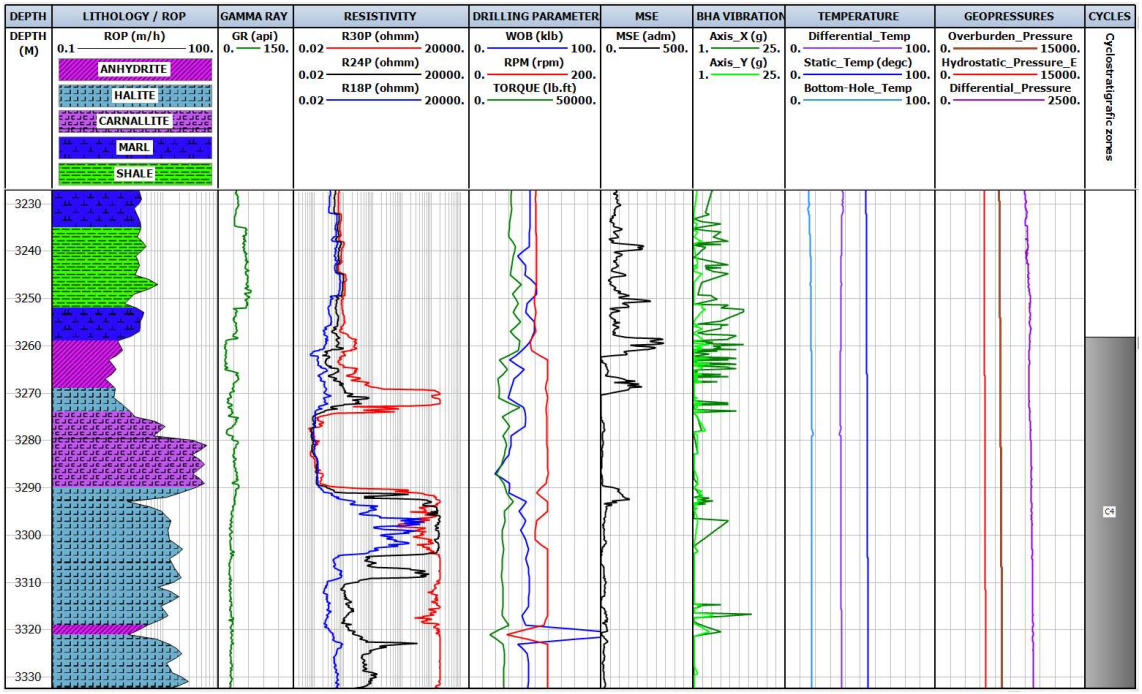

Figure 122. Log plot of the 3,230 to 3,330 m interval of the Wellbore 2, showing the dissolved layer of carnallite that was interpreted by the analyses of 18-, 24- and 30-inch 2-MHz Phase Resistivity investigation radii log response.

In-gauge borehole was considered when the 30-inch 2-MHz phase resistivity log shows very high values in the salt layers, as expected for a 26-inch drilling section. Washed-out borehole in halite and bittern salts were interpreted when the 30-inch 2-MHz phase resistivity log presented low values such as the logs of 18- and 24-inch radii, that are related to seawater low resistivity interference. Although enlargement gauge by salt dissolution also happens to halite layers, this occurs in a smaller scale because of their lower solubility than the bittern-salt solubility.

The borehole instability was also interpreted while drilling the 16-inch section using water-based NaCl-saturated drilling fluid. It was attributed to the salt creeping that caused severe BHA stuck in the C1 cycle producing a broken BHA with no possibility of recovery. It was necessary to abandon part of the borehole, deviate it, and start drilling again from that point on.

4.3. Wellbore 3

Borehole instability attributed to salt creeping caused severe BHA stuck in the C1 cycle while drilling the 16-inch section using oil-based drilling fluid.

4.4. Wellbore 4

Borehole instability attributed to salt creeping caused severe BHA stuck in the C1 cycle while drilling the 16-inch section using water-based NaCl-saturated drilling fluid.

4.5. Wellbore 5

Severe BHA stuck in the C1 cycle were attributed to salt creeping while drilling the 16-inch section using oil-based drilling fluid. It produced a broken BHA with no possibility of recovery. Thus, it was necessary to abandon part of the borehole, deviate it, and restart drilling. The same problem occurred repeatedly until reaching the base of the Ariri Formation.

4.6. Wellbore 6

Two severe events of BHA stuck in the C1 cycle were registered in an unstable borehole condition. They were interpreted as caused by salt creeping in a halite layer while drilling the 16-inch section using oil-based drilling fluid.

4.7. Wellbore 7

Borehole instability occurred first in the 26-inch section using seawater as drilling fluid. Impediments to run and installing the borehole casing across the 26-inch open well is a strong evidence of borehole closure by salt creeping. The borehole internal diameter was reduced during the time interval required to pull the drilling BHA out of the hole and run the case into the hole. To solve this problem, it was necessary to take the casing out of the borehole and run the 26-inch drilling BHA back inside to ream the restricted

intervals. Three main intervals of reduced gauge were detected while reaming close to the bottom hole. A vigorous flow of seawater was required to wash-out the borehole by dissolving the salts that were obstructing the case running. Basically, the success or failure of the adopted solution depends on which one of the following variables runs faster, salt dissolution or creeping.

Moreover, the most relevant occurrences of borehole instability were registered while drilling the 16-inch section, using water-based NaCl-saturated drilling fluid. A large volume of drilling fluid was lost to the formation since the beginning of this drilling section. This loss may be aggravated by a poor cementation at the 26-inch casing-shoe.

Fluid losses while drilling the 16-inch section impeded the increasing of the hydrostatic pressure inside the borehole. An undesirable effect of increasing the hydrostatic pressure is the aggravation of drilling-fluid losses in the region close to the 22-inch casing shoe. Therefore, the low hydrostatic pressure while drilling the 16-inch section resulted in a series of severe events of drilling BHA stuck associated to salt creeping in the C1 cycle that turned the drilling operations very costly and troublesome. The BHA broke with no possibility of recovery after the several attempts to release it. Part of the borehole had to be abandoned and deviated to continue drilling. After that, other occurrences of BHA stuck repeated several times. A solution of the problem required a reduction of the ROP and the pumping of seawater “pills” inside the borehole to dissolve the creeped salt.

4.8. Wellbore 8

Severe BHA stuck in the C1 cycle while drilling the 16-inch section using water-based NaCl-saturated drilling fluid was related to borehole instability caused by salt creeping. The solution of the problem required the use of drilling BHA Jar percussion tool and seawater “pills” to free the drilling BHA.

Figure 13 represents the interval of 4,150-5,450 meters of the 16-inch diameter of the Wellbore 8. A drastic increasing of the differential pressure at the bottom of C1 cycle is represented in track 8, as a decreasing of the differential temperature, in track 7. Elevated bottom-hole temperatures while drilling occurred in all those three events of BHA stuck. After that, it is possible to observe a BHT reduction by the drilling-fluid

circulation through the borehole. The differential temperature while drilling varies from 22°C to 35°C, and events of BHA stuck happened at low differential temperatures (red boxes in Figure 13, at depths of 4,621 m, 4,932 m, and 5,164 m).

An enormous difference between the resistivity logs of the 18- and 30-inch investigation radii are showed in Figure 13, track 4. It happens at the top section and was interpreted as an enlarged section where the rocks were dissolved by the drilling fluid. The low anomalous values presented by the 18-inch 2-MHz phase resistivity log are related to the effect of the drilling fluid resistivity. From middle to bottom section, the 18-inch 2-MHz phase resistivity log shows increasing values that approximate those of the 30-inch 2-MHz phase resistivity log representing a reduction of the borehole diameter and creating an in-gauge situation.

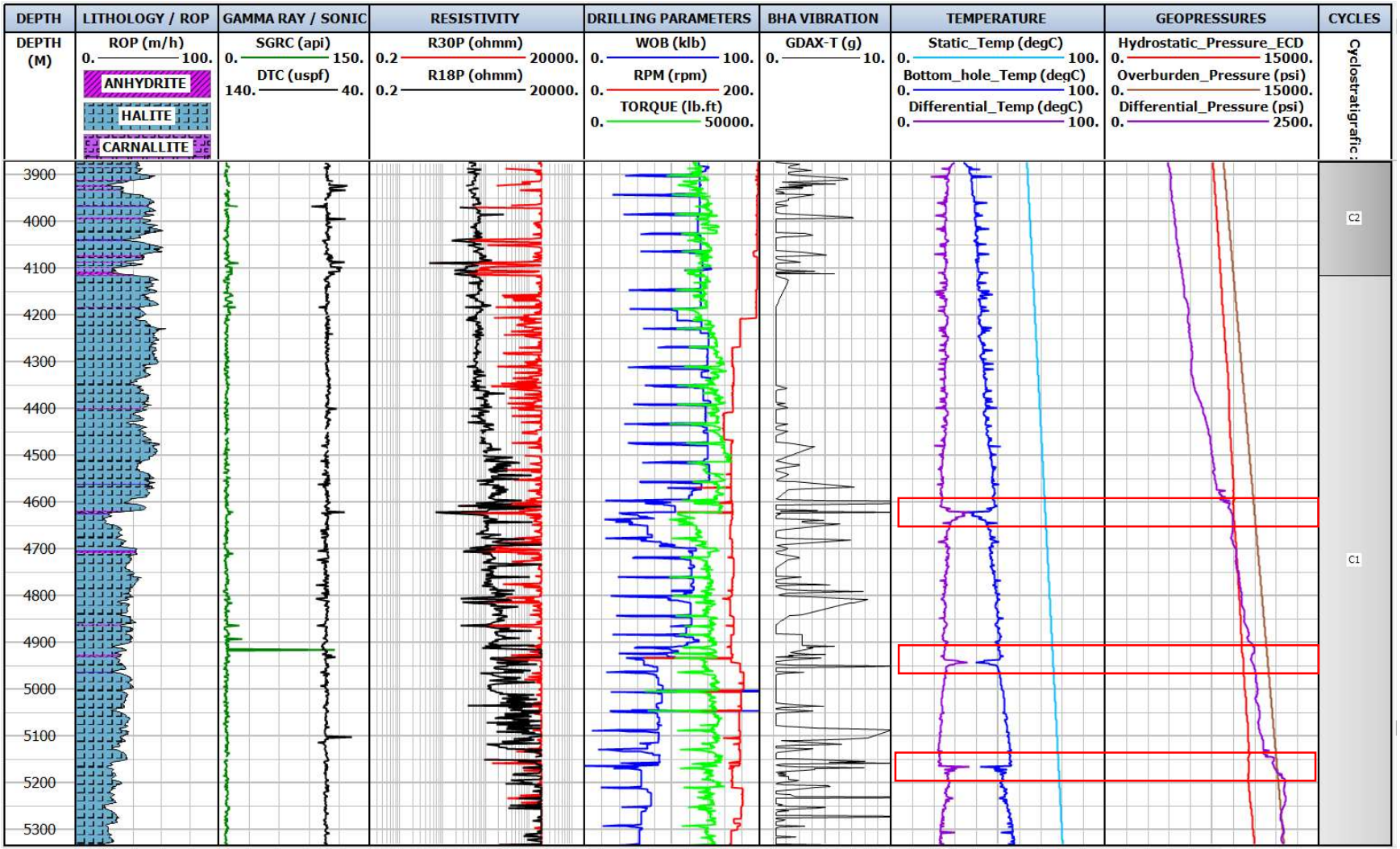

Figure 13. The red boxes show the interval of BHA stuck by salt creeping in the 16-inch section of the Wellbore 8.

Table 5 shows twenty events of BHA stuck by salt creeping in the selected wellbores, and their corresponding pressure and temperature conditions. The differential pressures vary from 1,368.45 psi to 2,635.29 psi and the differential temperature varies from 14.20 °C to 40.70 °C. The ratio between hydrostatic pressure and overburden pressure varies from 75.81 % to 88.32 % and temperature ratio between the bottom-hole and static-rock temperatures varies from 28.72% to 81.60%. Pressure ratio and the temperature ratio data were plotted on a Scatter Plot (Figure 14). The linear regression demonstrates a good relation between the variables and the standard deviation presents low values for those parameters. The result function can be used in further studies about the management of hydrostatic pressure and bottom-hole temperature for the borehole stability control under salt creeping.

WELLBORE	True Vertical Depth	Measured Depth	HP	OP	BHT	SRT	OP-HP	SRT-BHT	HP/OP	BHT/SRT
7	5,155	5,183	9,838	12,473	45.7	76.8	2,635	31.1	0.79	0.60
7	5,037	5,064	9,613	12,102	43.3	75.3	2,489	32.0	0.79	0.58
7	5,117	5,145	9,765	12,294	45.0	76.2	2,528	31.2	0.79	0.59
7	4,710	4,731	8,988	11,075	40.2	71.1	2,086	30.9	0.81	0.57
7	4,563	4,581	8,708	10,652	37.2	69.2	1,943	32.0	0.82	0.54
7	4,444	4,460	8,481	10,222	34.7	67.4	1,741	32.7	0.83	0.51
4	5,087	5,273	9,795	11,788	53.1	80.7	1,993	27.6	0.83	0.66
8	5,368	5,374	10,519	12,622	57.9	80.6	2,103	22.7	0.83	0.72
8	5,158	5,164	10,107	12,041	56.1	78.2	1,933	22.1	0.84	0.72
5	5,285	5,285	10,986	13,058	61.0	86.2	2,071	25.2	0.84	0.71
8	4,926	4,932	9,569	11,331	50.6	75.6	1,762	25.0	0.84	0.67
5	4,546	4,546	9,063	10,690	52.0	75.9	1,626	23.9	0.85	0.69
5	4,992	4,992	10,292	12,079	56.3	81.9	1,786	25.6	0.85	0.69
2	4,953	4,965	9,790	11,393	49.3	75.8	1,603	26.5	0.86	0.65
2	5,064	5,076	10,009	11,649	50.5	76.6	1,639	26.1	0.86	0.66
8	4,615	4,621	9,043	10,459	48.2	71.8	1,415	23.6	0.86	0.67
1	4,724	4,726	9,337	10,706	54.6	71.4	1,368	16.7	0.87	0.76
1	5,279	5,281	10,884	12,323	63.4	77.7	1,439	14.2	0.88	0.82
1	5,078	5,079	10,470	11,854	64.0	79.5	1,384	15.5	0.88	0.81

Table 5. Differential and ratio pressures and temperatures of each event of BHA stuck by salt creeping in the selected wellbores.

Based on descriptive statistics parameters, it is possible to state that the Hydrostatic/Overburden Pressure Ratio and the Bottom-hole/Static-Rock Temperature

Ratio data have low dispersion around the mean i.e. low standard deviation. Furthermore, the mean and median are close which suggests a symmetric distribution of data (Table 6).

	HP	OP	BHT	SRT	OP-HP	SRT-BHT	HP/OP	BHT/SRT
MEAN	9,507	11,362	49.0	75.3	1,855	26.3	0.84	**0.64**
STDV	1,285	1,401	11.2	6.2	381	6.4	0.03	**0.12**
MIN	4,882	6,439	16.4	57.1	1,368	14.2	0.76	**0.29**
25%	9,058	10,702	44.6	71.7	1,592	23.4	0.82	**0.59**
50%	9,777	11,719	50.5	76.0	1,774	25.8	0.84	**0.66**
75%	10,153	12,150	56.1	78.5	2,075	31.1	0.86	**0.71**
MAX	**10,986**	**13,058**	**64.0**	**86.2**	**2,635**	**40.7**	**0.88**	**0.82**

Table 6. Descriptive Statistics Parameters of the pressures and temperatures statistical analysis.

	HP	OP	BHT	SRT	OP-HP	SRT-BHT	HP/OP	BHT/SRT
HP	**1.00**	**0.96**	**0.91**	**0.92**	**0.17**	**-0.69**	**0.60**	**0.86**
OP	**0.96**	**1.00**	**0.79**	**0.91**	**0.43**	**-0.50**	**0.37**	**0.72**
BHT	**0.91**	**0.79**	**1.00**	**0.88**	**-0.15**	**-0.89**	**0.77**	**0.97**
SRT	**0.92**	**0.91**	**0.88**	**1.00**	**0.24**	**-0.56**	**0.47**	**0.77**
OP-HP	**0.17**	**0.43**	**-0.15**	**0.24**	**1.00**	**0.49**	**-0.67**	**-0.26**
SRT-BHT	**-0.69**	**-0.50**	**-0.89**	**-0.56**	**0.49**	**1.00**	**-0.89**	**-0.95**
HP/OP	**0.60**	**0.37**	**0.77**	**0.47**	**-0.67**	**-0.89**	**1.00**	**0.85**
BHT/SRT	**0.86**	**0.72**	**0.97**	**0.77**	**-0.26**	**-0.95**	**0.85**	**1.00**

Table 7. Correlation Matrix of the pressures and temperatures data. The black boxes show the good positive correlation of 0.85 between HP/OP vs BHT/SRT.

The coefficient of determination represented by R^2 is a statistical measure that explains the strength between two variables in the scatter plot. The HP/OP vs BHT/SRT model obtained an R^2 of 0.7231 which means that approximately 72.31% of the data variability can be explained by these adopted statistical model (Figure 14). It also indicates a good capacity to explain the variations in the data and suggests that is still a substantial portion that remains unexplained and needs improvement.

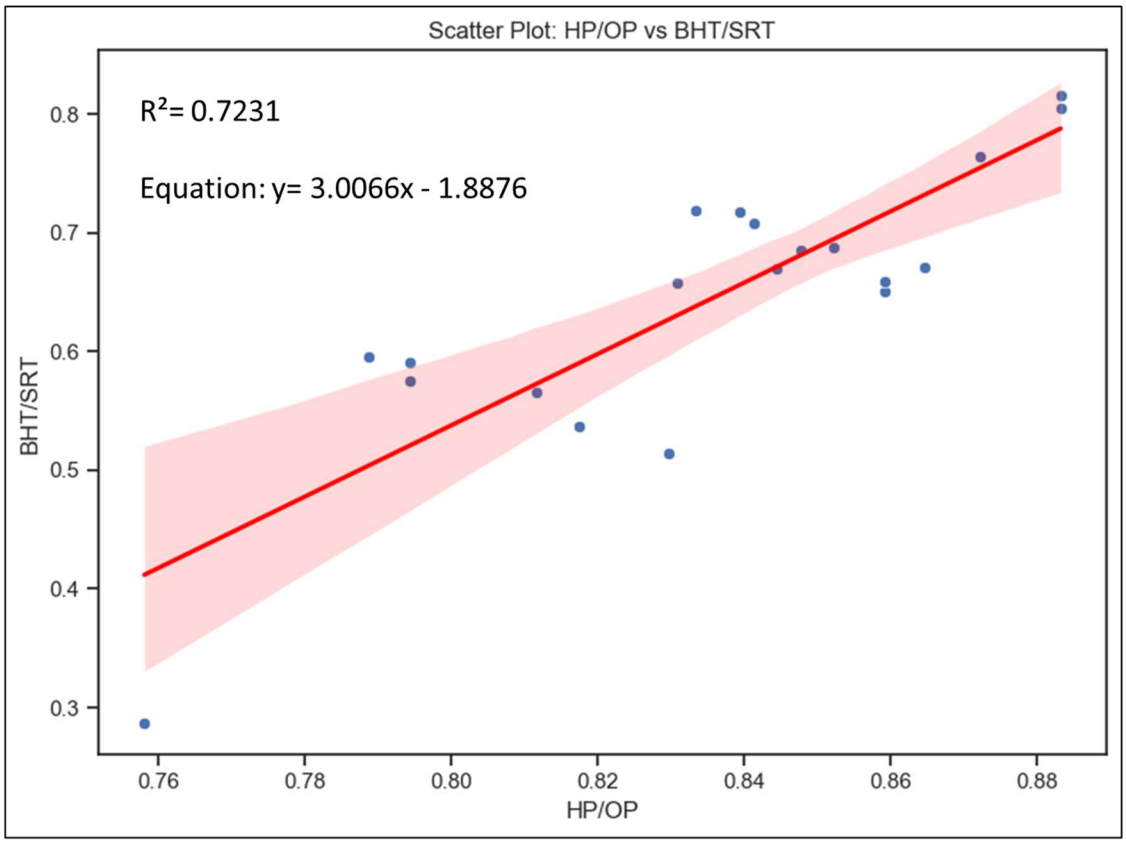

Figure 14. Pressure ratio versus temperature ratio in the Scatter Plot.

5. DISCUSSION

The stratigraphic analyses of these studies resemble those described by Teixeira et al. (2020) for the Ariri Formation in another similar area. Four major cycles of salt deposition, that is, concisely, thickened and halite-rich C1 cycle, C2 and C3 cycles similar lateral-continued layers, and C4 cycle enriched in anhydrite and bittern salts, presenting strong reflections, and strong diagenetic deformation. The seismic analysis show that seven wellbores are positioned in a high structure of the top salt surface, while only the Wellbore 3 is located in a low structure (Figure 5), that is filled by Albian carbonate of the Camburí Group (Figure 2). The Albian carbonate build-up in the basing seems to create an overburden load to the salt layers underneath the carbonate mini basin, mobilizing much of the halite of the C1 cycle. The C4 cycle is the most affected by the diagenesis, just because of its top position, which are directly subjected to the post-salt climatic alterations. The anhydrite enrichment of the C4 cycle can be related to a super-genetic enrichment because of its lower solubility and mobility than halite and bittern salts that are more subjected to climatic alterations.

The temperature gradient on salt rocks on all wellbores present a good correlation to Pestana et al. (2018). It varies from 10.5 to 13.5 °C/km on the wellbores (Table 4) and from 11 to 13 °C/km on Pestana et al. (2019). The SRT at the salt base of the selected wellbores do not exceed 107 °C, that is the convergence point where salt creeping increase abruptly (Le Comte, 1965). It varied from 77 to 85 °C (Table 4), where the salt creeping should occur in a small scale according to Le Comte (1965), Barker et al. (1994), and Moiseenkov et al. (2019) (Figure 4). The BHA stuck associated to salt creeping always occurs when the differential temperatures, i.e. SRT minus BHT are low (Figures 10 and Figure 13). The low differential temperature favored the salt creeping, and the reduction of the BHT after events of BHA stuck caused by a wide drilling fluid circulation at the bottom hole shows that the control of BHT is crucial to maintain borehole stability.

Deep wellbores have a telescopic shape and are split into sections with gradually reducing diameters (Triggia et al., 2004) in order to reach deep reservoirs below the salts of the Ariri Formation. Usually, there is no drilling fluid circulation to the rig platform in the two beginning sections of a wellbore and there are no sample rocks available for geologic analysis. On those sections, electrical well logs are also restricted due to the difference of the borehole-wall diameter and the 9-inch diameter of the logging tools that are unable to acquire good quality data. In the last drilling sections, when the borehole diameter is reduced, it is possible to establish the drilling-fluid circulation to the rig. The drilling-fluid circulation brings drilled-rock samples to the surface. A good quality control of the drilling-fluid volume and time of circulation through the entire system allows a good positioning of the cutting samples in a true depth to avail the geological analysis. Electrical well logs are more reliable in those last reduced-diameter sections due to the small difference between the diameter of borehole wall and the diameter of the logging tools.

Halite is easy to drill because of its low hardness. The ROP in halite layers is a parameter directly related to the management of the WOB, RPM, and flow rate of the drilling fluid. Usually there is no necessity to apply high WOB to have a good drilling performance in halite layers. When drilling halite layers, high RPM is a good option since it improves the reaming of the high-rate creeping deformation of the initial stage, which is known as transient state (Poiate, 2012). The rate of the creeping deformation rate reduces rapidly to a steady state. In the second stage of the salt-creeping, the deformation

rate is lower and constant. The high RPM helps ream the initial fast salt-creeping deformation and maintain the borehole gauge.

Electrical well logs are the principal input for the lithological interpretation of the rocks that are crossed by the boreholes. Lithological interpretations can be made using at least two electrical logs i.e. gamma ray and resistivity as referenced in the literature (Table 2), but the drilling parameters are also especially useful to support those interpretations. Unexpectedly, the gamma-ray log of carnallite layers in the selected wellbores show low values than expected. This happens in different conditions as, for example, in over-gauged boreholes that underwent salt dissolution, when the gamma ray log response is attenuated.

Anhydrite layers showed a large variation of resistivity values, not high as expected (Figure 11 and Figure 12). Low resistivity values were attributed to a mixing anhydrite, gypsum, and lutite, that is a silt- to clay-size sediment equivalent to mudstone or pelite (Guinea et al., 2012). According to Caselle et al. (2019), it can also be a response to the porosity and water content of calcium sulfates. Nevertheless, low resistivity values for anhydrite in the selected wellbores should not be interpreted as dissolved and enlarged layers, as was done for halite and bittern salts. Calcium-sulfate rocks dissolution does not occur as for halite and bittern salts since the solubility of calcium sulfate rocks is roughly 140 times lower than the solubility of halite (Klimchouk, 1996).

Considering the investigation radius of the 2-MHz phase resistivity tool as the distance from the sensors, which is measured perpendicularly to the drilling BHA, radii of 18-, 24-, 30- and 40-inch were used to evaluate qualitatively the integrity of the borehole diameter in bittern-salt and halite layers. Those salts are supposed to present high resistivity values (Table 3), but sometimes this does not occur. In a washed-out borehole, the drilling fluid fills the dissolved salt space, and the resistivity sensor provides the drilling-fluid resistivity response, rather than the salt formation response. The low resistivity anomaly of washed-out layers aggravates in bittern salts when seawater is used as the drilling fluid. Bittern salts have high potential for dissolution when non-saturated water-based drilling fluids are used. However, oil-based drilling fluid can reduce this effect.

Sonic logs can be used for the understanding of the low-resistivity layers of anhydrite (Figures 11 and 12). Sonic values for pure anhydrite should be close to 50 μs/ft

(Table 2). Nonetheless, some intervals of interpreted anhydrite layers presented different sonic values than those that are expected. They are always associated to low resistivity values. According to Guinea et al. (2012), this may indicate existence of a impure anhydrite possibly mixed with gypsum or/and lutite, or to a porous facies with some water content (Caselle et al., 2019).

Borehole enlargement by salt dissolution is one of the main causes of borehole instability in the Ariri Formation. Figure 12 shows the top of the C4 cycle in the Wellbore 2, where anomalous low resistivity values were registered in a 15-meter layer of carnallite when using seawater as the drilling fluid. This unexpected low resistivity values were attributed to the seawater, which is filling the enlarged borehole carnallite interval, in an unstable borehole condition. The seawater washed out the borehole walls, dissolved the highly-soluble carnallite, and enlarged uncontrollably the borehole gauge.

An in-gauge borehole condition for a 25m-thick layer of carnallite of the C3 cycle of the Wellbore 1 was interpreted using 2-MHz phase resistivity logs of different investigation radii (Figure 11), that present high values for all logs, and small variation among those values. That thick carnallite layer can represent a high potential risk for borehole instability because of the high-solubility and fast-creeping proprieties of that salt. Nonetheless, the low dissolution produced by the oil-based drilling fluid and the lower differential pressure contribute to the stability control of the wellbore in that carnallite layer.

The use of seawater as the drilling fluid to drill thick layers of tachyhydrite can cause the release of large volume of water from the internal structure of that mineral by dissolution. After finishing drilling and circulating the drilling fluid on the bottom hole the dissolution process reduces and The salt creeping resumes in the dissolved and enlarged section of the borehole, giving an influx-like semblance.

The main cause of borehole instability in all studied cases is related to salt creeping, which is the cause of the BHA stuck. This happens when HP is much lower than OP, which produces high differential pressure, and the BHT is close to SRT, which results in a low differential pressure, as shown in Figures 10 and 13. That usually occurs at the base of the C1 cycle, near the contact of the Ariri and Barra Velha Formations, when the increase of HP is restricted.

Salt creeping depends mostly on differential pressures (Overburden Pressure minus Hydrostatic Pressure), differential temperature (rock static temperature minus bottom-hole internal temperature), drilling fluid characteristics, and salt type. When the hydrostatic pressure is lower than the overburden pressure, salt can creep into the borehole, reducing its internal diameter (Moiseenkov et al., 2019). When the drilling fluid temperature at the bottom hole increases the differential temperature reduces, and the creeping rate can also increase.

Data analyses show that drilling under salt-creeping conditions for a long time can wear and damage the drilling tools, produce poor data and, in some cases, break the drilling string. This last situation is the worst scenario. In such a situation, it is necessary to either employ a fishing tool or abandon the affected interval of the borehole, deviate it, and resume drilling. Salt creeping also occur when the differential temperature at the bottom-hole is increased by the application of high WOB, RPM, and flow rate of the drilling fluid.

The use of seawater to drill the 26-inch section of the Wellbore 7 was responsible for a low HP inside the borehole. The higher OP gradient increases the differential pressure between the HP and OP as the depth increases. Such a condition aggravates the possibility of salt creeping. Even so, after stopping drilling the 26-inch section, the BHT increases and tends to equal the RST. This happens because of the end of the refreshment given by the fluid circulation at the bottom hole.

Impediments to run the borehole casing of Wellbore 7 across a halite layer after finishing drilling the 26-inch section are physical evidence of the creeping effect. The difficulty of installing the casing in that hole is a convincing evidence of borehole closure by salt creeping. The casing had an outside diameter of 22 inches and the borehole had an internal diameter of 26 inches. This means that the salt creeping reduced the borehole internal diameter of at least 4 inches during the time interval between pulling the drilling BHA out of the hole and running the case into the hole. To solve this problem, it was necessary to take the casing out of the borehole and run the 26-inch drilling BHA back inside to ream the affected intervals. Three intervals of reduced gauge were detected while reaming close to the bottom hole. A vigorous flow of seawater was applied to wash-out the borehole by dissolving the salts. Basically, the success or failure of the adopted

solution depends on which one of the following variables runs faster, salt dissolution or creeping.

Large losses of drilling fluid occurred while drilling the 16-inch section of the Wellbore 7, which can be caused by a poor cementation at the 22-inch casing-shoe. The reaming operation of the 26-inch section using seawater as the drilling fluid enlarged uncontrollably the borehole, turning the cementing operation more difficult. The occurrence of bittern-salt layers close to the bottom hole can increase the enlargement process. Fluid losses while drilling the 16-inch section impeded the increasing of the hydrostatic pressure and salt creeping that caused a series of events of drilling BHA stuck events and turning the drilling operations very costly and troublesome.

A drastic increasing of the differential pressure at the bottom of the C1 cycle while drilling the 16-inch section of the Wellbore 8 using water-based NaCl-saturated drilling fluid caused several events of BHA stuck in halite layers as well, which were attributed to salt creeping (Figure 13). The high differential pressure ultimately reduced the borehole diameter which caused an unusual work of the drilling components above the bit, including stabilizers, roller-reamers, and reamers. In addition, it is possible to associate an aggravation of BHA vibration while drilling halite with the events of BHA stuck by salt creeping. These conditions can also elevate the temperature of the BHA tools and the bottom-hole drilling fluid temperature increasing, as a consequence, the risk of salt creeping.

Low fracture pressure at the top of the drilling section was prevents the increasing of the HP while drilling the last 1,000 meters of the Ariri Formation in the Wellbore 8 (Figure 13). Low HP facilitates the occurrence of salt creeping that is ultimately the cause of BHA stuck. The solution of the problem required the use of drilling BHA Jar percussion tool and seawater “pills” to free the drilling BHA.

Usually, the main way to control salt creeping and avoid borehole instability is by increasing the HP. But there are limits, the low fracture pressure in the top of the Barra Velha Formation creates a high-risk condition for rock fracturing while exiting the Ariri Formation. On that circumstance, drilling fluid losses and other related problems may occur. Nevertheless, drilling fluid losses related to rubble zones or karstic features while

exiting the salt section, at the Ariri-Barra Velha contact, were not detected in all selected wellbores.

The differential temperature, i.e. SRT minus BHT is another parameter to be considered in borehole stability control when salt-creeping conditions potentially exist. In Figures 10 and 13 it is possible to observe that the refreshment, which is produced by the drilling fluid circulation through the borehole, reduces the BHT while drilling after events of BHA stuck. The differential temperature while drilling varies from 22°C to 35°C, and events of BHA stuck happened at low differential temperatures (red boxes in Figure 10, at depths 4,621 m, 4,932 m, and 5,164 m). Elevated bottom-hole temperatures while drilling occurred in those three events of BHA stuck. BHT reduction by drilling fluid circulation under conditions of no drilling progression was enough to increase the differential temperature and reestablish the stability of the borehole after those events of BHA stuck referred to above.

6. CONCLUSIONS

The stratigraphy study of the Ariri Formation allowed the identification of four major cycles in the selected seismic section. These cycles were named C1, C2, C3 and C4 from bottom to top of the Ariri Formation. C1 is the thickest cycle and was most thickened by halokinetic deformation. It is rich in halite and presents seismic transparent to chaotical facies because of its low-interbedded layers of other salts. The C2 and C3 cycles are very similar. They are thinner and present strong signal of interbedded layers, which are caused by anhydrite and bittern-salt intercalations. The C4 cycle shows the largest amount of anhydrite and bittern salts. It has strong reflections and chaotical seismic facies that are associated to intense halokinetic deformation and strong diagenetic process. It is important to mention that bittern salts occur in the four mapped cycles. Even in the C1 cycle, it occurs as a 25-m thick layer of carnallite in the Wellbore 1. This layer is close to the top of the C1 cycle and above thick halite section.

Drilling geomechanics analyses show that salt creeping is the main cause of borehole instability in the Ariri Formation. It happens when the differential pressure, which is the overburden pressure minus the hydrostatic pressure, increases. This occurs mostly in the C1 cycle. In such a condition, the hydrostatic pressure must be kept low to avoid the risks of damaging the casing shoe that was installed previously or fracturing the

carbonate rocks of the Barra Velha Formation. In addition, the existence of karstic features or ruble zones aggravates the picture. Salt creeping reduces the internal diameter of the borehole and causes BHA stuck while drilling. This is responsible for a lot of non-productive time that inflates costs of a wellbore construction. Usually, the BHA stuck demands the use of seawater “pills” to dissolve the salt and release the BHA. It is also common the use of the drilling jar percussion tool to free the BHA and resume drilling.

Events of BHA stuck by salt creeping while drilling the Ariri Formation were individually characterized in these studies. Twenty-two events of BHA stuck were registered in the selected wellbores. A pressure versus temperature Scatter Plot was drawn to compare the pressure ratio (ratio of HP over OP) and the temperature ratio (ratio of BHT over SRT) of each event. A linear regression was traced using 20 data points. Its resultant function can be used in further studies for borehole-stability control and drilling management of pressures and temperatures to control salt creeping. When HP cannot be increased due to the mentioned risks, the reduction of BHT must be as a procedure to the control of salt creeping. This is achieved by reducing the ROP and increasing the drilling-fluid flow rate at the bottom hole. In addition, the salt saturation of the drilling fluid also affects the borehole stability in salt formations.

Uncontrolled enlargement by the use of non-saturated water in the drilling fluid can also cause borehole instability. The dissolution process of bittern salts must be carefully observed for borehole control. The 2-MHz Phase resistivity logs can be useful to certify the borehole caliper gauge. This analysis can be very important when seawater is used as the drilling fluid because of its high potential for dissolution of halite and bittern salts. When using seawater as the drilling fluid, the high differential pressure can increase the possibility of salt creeping. The dissolution and creeping processes in bittern-salt layers can produce water influxes and poor casing cementation.

It is important to emphasize the importance of seismic processing using new inversion algorithms as proposed by Yamamoto (2019), Teixeira et al. (2020), and Maul et al. (2021) to minimize ambiguity in the amplitude response, refine the seismic facies classification and the geological interpretation of bittern-salt and anhydrite layers in the Ariri Formation.

7. REFERENCES

Alves T. M., Fetter M., Lima C., Cartwright J.A., Cosgrove J., Gangá A., Queiroz C.L., Strugale M. 2017. An incomplete correlation between pre-salt topography, top reservoir erosion, and salt deformation in deep-water Santos Basin (SE Brazil). Marine and Petroleum Geology 79: 300-320. https://doi.org/10.1016/j.marpetgeo.2016.10.015

Aslanian D., Moulin M., Olivet J.-L., Unternehr P., Matias L., Bache F., Rabineau M., Nouzé H., Klingelhoefer F., Contrucci I., Labails C., 2009. Brazilian and African passive margins of the central segment of the south Atlantic ocean: kinematic constraints. Tectonophysics (Special Issue: role of magmatism) 468, 98–112.

Barker J.K., Feland K.W., Tsao Y-H. 1994. Drilling Long Salt Sections Along the U.S. Gulf Coast. SPE Drilling & Completion. September-1994: 185-188. https://doi.org/10.2118/24605-PA

Caselle C., Bonetto S., Comina C. 2019. Comparison of laboratory and field electrical resistivity measurements of a gypsum rock for mining prospection applications. International Journal of Mining Science and Technology. 29: 841–849. https://doi.org/10.1016/j.ijmst.2019.09.002

Carrapatoso, C. M. 2011. Análise dos modelos analíticos de otimização de perfuração baseados em energia específica para formações evaporíticas. Master's thesis. Universidade Federal Fluminense: 1-164. https://doi.org/10.17771/PUCRio.acad.17928

Clauzon G., Suc J.-P., Gautier F., Berger A., Loutre M.-F. 1996. Alternate interpretation of the Messinian salinity crisis: controversy resolved? Geology. 24 (4): 363–366. Geology (1996) 24 (4): 363–366. https://doi.org/10.1130/0091-7613(1996)024<0363:AIOTMS>2.3.CO;2

Costa A.M., Poiate Jr E., Amaral C.S., Gonçalves C.J.C., Falcão J.L. 2010. Geomechanics applied to the well design through salt layers in Brazil: A History of success. 44th U.S. Rock Mechanics Symposium and 5th U.S. Canada Rock Mechanics Symposium. American Rock Mechanics Association. ARMA-10-239: 1-13.

Davison I., Anderson L., Nuttall P. 2012. Salt deposition, loading and gravity drainage in the Campos and Santos salt basins. Salt Tectonics. Sediments and Prospectivity - Geological Society Special Publications. (363) 159–174. https://doi.org/10.1144/SP363.8

Dusseault M.B., Maury V., Sanfilippo F., Santarelli F.J. 2004. Drilling Through Salt: Constitutive Behavior and Drilling Strategies. 6th North America Rock Mechanics Symposium (NARMS): Rock Mechanics Across Borders and Disciplines. American Rock Mechanics Association. ARMA 04-608: 1-13.

Falcão L. F. 2017. O sal estratificado e sua importância na modelagem de velocidades para fins de migração sísmica. Masters in science thesis. Universidade Federal Fluminense. 93p. https://doi.org/10.13140/RG.,2.2.24457.49768

Farias F., Szatmari P., Bahniuk A., França A.B. 2019. Evaporitic carbonates in the pre-salt of Santos Basin - genesis and tectonic implications. Marine and Petroleum Geology. 105: 251-272. https://doi.org/10.1016/j.marpetgeo.2019.04.020

Fiduk J.C., Rowan M.G. 2012. Analysis of folding and deformation within layered evaporites in blocks BM-S-8 &-9. Santos Basin. Brazil. Salt Tectonics. Sediments and Prospectivity - Geological Society Special Publications. (363): 471–487. https://doi.org/10.1144/SP363.22

Fonseca J., Bulcão A., Dias B., Teixeira L., Maul A., Borges F. 2019. Combination of the salt stratifications and the least-square migration to evaluate their improvements for the pre-salt reservoir images in the Santos Basin. Brazilian offshore. 16th International Congress of the Brazilian Geophysical Society. Brazilian Geophysical Society: 1-4. https://doi.org/10.22564/16cisbgf2019.083

Freitas J.R. 2006. Ciclos deposicionais evaporíticos da Bacia de Santos: uma análise cicloestratigráfica a partir de dados de 2 poços e traços de sísmica. Masters in science thesis. Universidade Federal do Rio Grande do Sul. 168p.

Gamboa L.P., Machado M., da Silveira D., de Freitas J., da Silva S. 2009. Evaporitos estratificados no Atlântico Sul: interpretação sísmica e controle tectono-

estratigráfico na Bacia de Santos. Sal: Geologia e Tectônica. Exemplos nas Bacias Brasileiras: 342-361.

Garcia S.F.M., Letouzey J., Rudkiewicz J.L., Filho A.D., de Lamotte D.F. 2012. Structural modeling based on sequential restoration of gravitational salt deformation in the Santos Basin (Brazil). Marine and Petroleum Geology. 35 (1): 337-353. https://doi.org/10.1016/j.marpetgeo.2012.02.009

Gomes. P. O., Kilsdonk. W., Grow. T., Minken. J. & Barragan. R. 2012. Tectonic evolution of the outer high of the Santos Basin. southern São Paulo Plateau. Brazil. and implications for hydrocarbon exploration. Tectonics and Sedimentation - Implications for Petroleum Systems. American Association of Petroleum Geologists Memoirs. (100): 125–142. https://doi.org/10.1306/13351550M1003530

Guinea A., Playa E., Rivero L., Ledo J.J. Queralt P. 2012. The electrical properties of calcium sulfate rocks from decametric to micrometric scale. Journal of Applied Geophysics. (85): 80–91. https://doi.org/10.1016/j.jappgeo.2012.07.003

Imbert. P., Yann. P. 2005. The Mesozoic opening of the Gulf Coast of Mexico: Part 2: Integrating seismic and magnetic data into a general opening model. Petroleum Systems of Divergent Continental Margin Basins - 25th Annual Bob F. Perkins Conference: 1151–1189. https://doi.org/10.5724/gcs.05.25.1151

Jackson C.A.L., Cramez C., Fonck J. 2000. Role of subaerial volcanic rocks and mantle plumes in creation of South American margins: implications for salt tectonics and source rocks. Marine and Petroleum Geology. (17): 477-498. https://doi.org/10.1016/S0264-8172(00)00006-4

Jackson C.A.L., Jackson M.P., Hudec M.R., Rodriguez C.R. 2015. Enigmatic structures within salt walls of the Santos Basin - part 1: Geometry and kinematics from 3d seismic reflection and well data. Journal of Structural Geology. (75): 135-162. https://doi.org/10.1016/j.jsg.2015.01.010

Jackson. M.P.A., Hudec. M.R. 2017. Salt Tectonics. Cambridge University Press. https://doi.org/10.1017/9781139003988

Logan. B. W. 1987. The Macleod evaporite Basin. Western Australia. Holocene environments. sediments and geological evolution. American Association of Petroleum Geologists Special Volume. (44): 132–133. https://doi.org/10.1306/M44465

Klimchouk. A. 1996. The dissolution and conversion of gypsum and anhydrite. International Journal of Speleology. 25 (3-4): 21-36. https://doi.org/10.5038/1827-806X.25.3.2

Kusznir N.J., Karner G.D., 2007. Continental lithospheric thinning and breakup in response to upwelling divergent mantle flow: applications to the Woodlark, Newfoundland and Iberia margins. In: Karner, G.D., Manatschal, G., Pihero, L.M. (Eds.), Imaging, Mapping and Modelling Continental Lithosphere Extension and Breakup. vol. 282. Geological Society of London Special Publications, pp. 389–419.

Le Comte. P. 1965. Creep in Rock Salt. The Journal of Geology. 73 (3): 469-484 https://doi.org/10.1086/627078

Lomba R.F.T., Teixeira G.T., Pessanha R.R., Lomba B.S., Folsta M.G., Cardoso Jr W.F., Gonçalves J.T. 2013. Lessons learned in drilling pre-salt wells with based muds. Offshore Technology Conference (OTC 24355-MS): 1:11. https://doi.org/10.4043/24355-MS

Marques F. S. B. 2019. Classificação Dinâmica Para o Evento de Prisão de Coluna na Perfuração de Poços Offshore. Master's thesis. Universidade Federal Fluminense: 1-105.

Maul A.R., Cetale. M.A., Guizan. C., Fonseca. J.S., Gonzales. M., Teixeira. L., Yamamoto. T.M., Borges. F.A.S., Pontes. R.L.B. 2019. Geological Characterization of Evaporitic Sections and its Impacts on Seismic Images: Santos Basin. Offshore Brazil. Revista Brasileira de Geofísica. 37(1): 55-68. http://dx.doi.org/10.22564/rbgf.v37i1.1989

Maul A.R., 2020. Caracterização sísmica das estratificações da seção Evaporítica salina e suas aplicações nos projetos de Exploração, desenvolvimento e produção de Hidrocarbonetos. Doctorate in science thesis. Programa de Pós-graduação em Dinâmica dos Oceanos e da Terra. 263p. http://dx.doi.org/10.13140/RG.2.2.19715.53285

Maul A.R., Cetale. M.A., Guizan. C., Corbett P., Underhill J.R., Teixeira L., Pontes R., González M. 2021. The impact of heterogeneous salt velocity models on the gross rock volume estimation: an example from the Santos Basin pre-salt, Brazil. Petroleum Geoscience. https://doi.org/10.1144/petgeo2020-105

Mohriak W., Szatmari P. (2009) Introdução às propriedades químicas e físicas dos evaporitos. Sal: Geologia e Tectônica, 19–41.

Moiseenkov A., Smirnov, D., Mahajan S., Al Hadhrami A., Al Azizi, I., Shabibi H., Balushi, Y., Omairi, M., Rashdi, M. 2019. Salt Creeping Effect on Borehole Collapse and Well Completion Design, Based on South Oman Field Experience. Society of Petroleum Engineers (SPE-197692-MS).

Montaron B., Tapponier P. 2010. A quantitative model for salt deposition in actively spreading basins. AAPG International Conference and Exhibition. (Article 30117): 1-8. https://doi.org/10.13140/RG.2.1.4078.8000

Moreira J. L. P., Madeira C.V., Gil J.A., Machado M.A.P. 2007. Bacia de Santos. Boletim de Geociências da PETROBRAS. 15(1): 531-549.

Moulin M., Aslanian D., Unternher P., 2010. A new starting point for the south and equatorial Atlantic Ocean. Earth Sci. Rev. 97 (Issues1–4), 59–95.

Oliveira L. C., Fernandes L. F., Maul A. R., Rosseto J. A. Farias M. L. A. G., Sanches G.G. 2015. Geological Velocity Approach in Order to Obtain a Detailed Velocity Model for the Evaporitic Section – Santos Basin. 14th International Congress of the Brazilian Geophysical Society. https://doi.org/10.1190/sbgf2015-273

Pereira M.J., Feijó F.J., 1994. Bacia de Santos. Estratigrafia das Bacias Sedimentares do Brasil. Bol. Geociências Petrobras 8, 219–234.

Pereira M.J., Macedo J.M., 1990. A Bacia de Santos: perspectivas de uma nova província petrolífera na plataforma continental sudeste brasileira. Bol. Geociências Petrobras 4, 3–11.

Pestana S. L., Guiza C. H. N., Pimentel N., 2018. Present-day thermal regime of the Santos Basin. Brazil. AAPG Europe Regional Conference. http://hdl.handle.net/10451/33940

Poiate Jr. E., Costa A.M., Falcao J. L., 2006. Well Design for Drilling Through Thick Evaporite Layers in Santos Basin – Brazil. IADC/SPE Drilling Conference (IADC/SPE 99161). https://doi.org/10.2118/99161-MS

Poiate Jr. E. 2012. Mecânica das rochas e mecânica computacional para projeto de poços de petróleo em zonas de sal. Doctorate in science thesis. Pontifícia Universidade Católica do Rio de Janeiro. 462p.

Pontes R. 2019. Seismic characterization of internal salt cycles: a case study in Santos Basin. Brazil. Master's thesis. Universidade Federal Fluminense: 1-36. https://doi.org/10.13140/RG.2.2.15188.22405

Pontes R., Maul A. R., Guizan C. 2021. Seismic Characterization of Internal Salt Cycles: remarks from the Santos Offshore Basin, Southeast Brazil. Seventeenth International Congress of the Brazilian Geophysical Society.

Rodriguez C., Jackson C.L., Rotevatn A., Bell R., Francis M. 2018. Dual tectonic-climatic controls on salt giant deposition in the Santos Basin. offshore Brazil. Geosphere. 14: 215-242. https://doi.org/10.1130/ges01434.1

Simpson D. A. 2017. Practical Onshore Gas Field Engineering. Chapter Two: Well-Bore Construction (Drilling and Completions). Gulf Professional Publishing, 85-134. https://doi.org/10.1016/B978-0-12-813022-3.00002-X.

Szatmari P., Milani E.J. 2016. Tectonic control of the oil-rich large igneouscarbonate-salt province of the South Atlantic rift. Marine and Petroleum Geology. 77: 567–596. https://doi.org/10.1016/j.marpetgeo.2016.06.004

Szatmari. P., de Lima. C.M., Fontaneta. G., Lima. N. de M., Zambonato. E., Menezes. M.R., Bahniuk. J., Coelho. S.L., Figueiredo. M., Florencio. C.P., Gontijo. R. 2021. Petrography. geochemistry and origin of South Atlantic evaporites: The Brazilian

side. Marine and Petroleum Geology. 127: 31p.https://doi.org/10.1016/j.marpetgeo.2020.104805

Tavares R. M. 2006. Interpretação e Análise de Dados de Perfuração em Poços de Petróleo. Master's thesis. Universidade Estadual de Campinas: 1-145.

Teale R., 1965. The concept of specific energy in rock drilling. International Journal of Rock Mechanics and Mining Sciences & Geomechanics Abstracts. 2(1): 57-73. https://doi.org/10.1016/0148-9062(65)90022-7

Teixeira L., Lupinacci W.M., Maul A. 2020. Quantitative seismic-stratigraphic interpretation of the evaporite sequence in the Santos Basin. Marine and Petroleum Geology. 122: 17p. https://doi.org/10.1016/j.marpetgeo.2020.104690

Triggia A.A., Correia C.A., Filho C. V., Xavier J.A.D., Machado J. C.V., Thomaz J. E., Filho J.E.S., Paula J. L., DeRossi N.C.M., Pitombo N.E.S., Gouvea P.C.V.M., Carvalho R.S., Barragan R.V. 2004. Fundamentos de engenharia de petróleo. Editora Interciência. 2ª Edição.

Warren J., 2006. Evaporites: Sediments. Resources and Hydrocarbons. Springer.

Whitfill D., Rachal G., Lawson J. 2002. Drilling Salt – Effect of Drilling Fluid on Penetration Rate and Hole Size. SPE Drilling Conference (IADC/SPE 74546): 1-8. https://doi.org/10.2118/87216-PA

Widess, M., 1973. How thin is a thin bed? Geophysics 38 (6), 1176–1180. https://doi.
org/10.1190/1.1440403

Yamamoto T.M. 2019. Uma metodologia para a caracterização da formação ariri utilizando dados de poços e inversão sísmica. Masters in science thesis. Universidade Federal Fluminense. 127p. https://doi.org/10.13140/RG.2.2.34670.15686